Tampere University

Trieu Quang Huy

FAULT DETECTION AND PREDICTION IN ELEVATORS USING FFT-BASED FEATURES

ABSTRACT

Trieu Quang Huy: Fault detection and prediction in elevators using FFT-based features
Master of Science Thesis
Tampere University
Science and Engineering, Theoretical Computer Science
May 2019

The purpose of this study is to find out how Fast Fourier Transform (FFT) based features could be used in fault detection and prediction in elevators. The overall main objective is to improve on the existing maintenance systems.

The data we analyzed in this work were obtained through applying FFT on vertical vibration signal of each elevator movement. The goal was to study the trend of data over time and detect any significant change that can indicate potential faulty behaviors inside elevators. Due to the challenges in analyzing a stream of high-dimensional FFT data, we decided to utilize two dimensionality reduction techniques, namely Feature selection with Dominant frequencies analysis and Feature extraction with Autoencoder. After that, we used change point detection on the newly acquired features to detect significant changes.

For validation, we first observed the FFT spectrum of each elevator and singled out the ones that contain clear visual changes. For these elevators, we estimated the visual change points and had them as the *target outputs* for our algorithms. The goal was to see if our implementation of feature selection and feature extraction, combined with change point detection could correctly the *target change points*.

Final results showed that all significant visual changes in the original spectrums could be detected through the use of feature selection and feature extraction, together with change point detection. Furthermore, we were able to calculate the percentage change in mean vibration amplitude of elevators to determine the most problematic cases with high increases in vibration level. These findings indicated that FFT based features can be used in identifying potential faulty behaviors in elevator systems and the techniques used in this work have shown promising results.

Keywords: *Elevators, Vibration analysis, Fast Fourier Transform, Feature selection, Dominant frequencies analysis, Feature extraction, Autoencoder, Change point detection*

PREFACE

This work is the result of an 8-month research in the Unit of Automation Technology and Mechanical Engineering from Tampere University (Formerly known as Tampere University of Technology). The name of the project that I was involved in is OPENS Novel Predictive Analytics Technologies for Future Maintenance Business.

First and foremost, I would like to express my sincere gratitude to Daniel Šutaj and Tapio Elomaa, my supervisors for the time and the support that they have given me. Without their assistance, I would not be able to finish my thesis in time. They were also very patient in dealing with my stubbornness, and thanks to them, I have learned a lot, not only on the academic aspect but also in life lessons.

Thanks to everyone from OPENS project for their advice and comments on my work. Special thanks to Tomi Krogerus for giving me the chance to be in OPENS. I hope that everything will go smoothly for you in your new workplace.

Finally, I would like to thank my parents, Trieu Duc Chinh and Nguyen Thi Hai, for their continuous encouragement throughout my life. Their words have always given me strength, no matter what hardship I may be going through. I hope that they can be proud of me.

Tampere, 03 May 2019

Trieu Quang Huy

CONTENTS

LIST OF FIGURES

LIST OF SYMBOLS AND ABBREVIATIONS

FFT	Fast Fourier Transform
DFT	Discrete Fourier Transform
DSP	Digital Signal Processing
SRS	Stanford Research Systems
PCA	Principal Component Analysis
ANN	Artificial Neural Network
FFNN	Feed-forward Neural Network
MLP	Multilayer Perception
DC	The zero bin (0Hz)
MATLAB	Multi-paradigm numerical computing environment and proprietary programming language

1. INTRODUCTION

Globally, there are more than 50% of the population living in urban rather than rural areas. In just under 70 years from 1950 to 2018, the number of people living in these areas has gone from 751 million to 4.2 billion and it shows no sign of stopping. By the year 2050, the global urban population is expected to increase by another 2.5 billion [1]. With increased global urbanization comes the increase in demands for supporting infrastructure. Due to this phenomenon, the elevator and escalator business has also experienced its own growth as well. For reference, in just Canada and the United States alone, 325 million passengers are estimated to use elevator services per day [2]. It is predicted that the market will continue to increase in size in the upcoming years, from 88.78 billion USD to 125.22 billion USD during the period of 2015-2021 [3].

Maintenance plays an important role in the elevator business model and income of the company, as a maintenance contract generate returns throughout the life-time of an elevator. However, the actual revenue is getting smaller because of the manual labor cost, which is mostly on-site inspection. A system that helps to reduce the frequency of these visits would definitely increase the revenue and be beneficial to the company in charge.

Maintenance strategies are often categorized into three main groups:

- **Corrective maintenance** which happens when the elevator system has already failed and personnel has to be sent out to fix or replace the broken components.
- **Preventive maintenance** is when on-site visits and check-ups happen regularly, with the aim is to detect problems early and prevent the system from failing.
- **Predictive maintenance**, on the other hand, tries to detect and predict problems through monitoring the condition of equipment using sensor data.

Due to the technological advancements in sensor technology, predictive maintenance, compared to other strategies, can more efficiently maximize the uptime, prolong the service life, cut repair costs and improve the stability of elevator systems [4]. As a result, it is now becoming the current trend in the elevator industry, in order to adapt the existing maintenance systems to meet the demands of the future [5].

In predictive maintenance, information about elevators, with parameters like acceleration, temperature, etc., are captured and reported through sensor systems in order to keep track of the condition of the machine. When the elevator starts showing signs of defect, behaves differently than normal, reflected by the changes in numbers of different parameters. If these

changes are detected early, the maintenance team can come to the site and potentially fix the problem before it becomes more serious. There are different techniques in data processing that can be used to fulfill this task and one such technique is **Fast Fourier Transform** (**FFT**).

FFT is a powerful tool which can transform time-series signal into frequency domain and using FFT in monitoring and maintaining rotating machine systems is a topic that has been studied extensively over the years [6] [7] [8]. For these systems, each rotating component with different characteristics can produce a different level of vibration that can vary depending on the health status of the machines. Using FFT analysts can not only detect the abnormalities with these components but also reliably diagnose the exact defects that they can have like unbalance, misalignment, looseness [7]. As an elevator system is comprised of a series of vibrating components, as can be seen from Figure 1, it is highly interesting to see how FFT can be used in monitoring elevators systems.
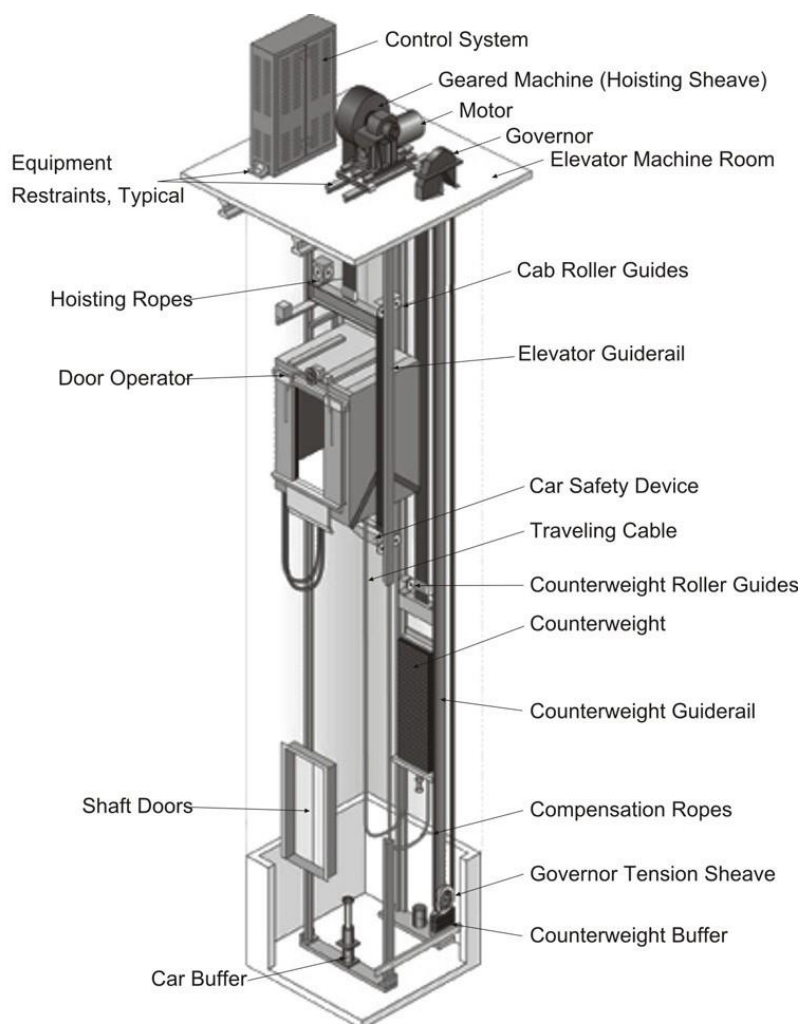
Figure 1. *The model of a modern traction elevator.*

The main task of this thesis is to analyze features that arise from applying FFT on raw sensor data in order to understand how it can be used in monitoring and maintaining elevators systems. FFT has been widely utilized in elevators vibration analysis [9] [10], however, these studies focused more on analyzing specific faults inside the elevator systems like with rotating machines. In this work, we approach the problem in a more general way and try to differentiate between healthy and faulty behaviors of elevators over time instead. The process involved reading a stream of FFT data and detecting abrupt changes, if any, in vibration amplitude. This can potentially indicate the transition between healthy (low amplitude) and faulty (high amplitude) states of elevators. Afterward, we also evaluate how much the vibration amplitude increase to find out the most problematic cases among a large population of elevators.

In this work, we try to answer a question that contributes to a more general overall problem, which is the improvement of the elevator maintenance system. Figure 2 illustrates a model of continuous iteration, where related knowledge and information are included, as a general approach toward solving the problem. This study focuses on the research aspect of the model, which is indicated by the red rectangle.
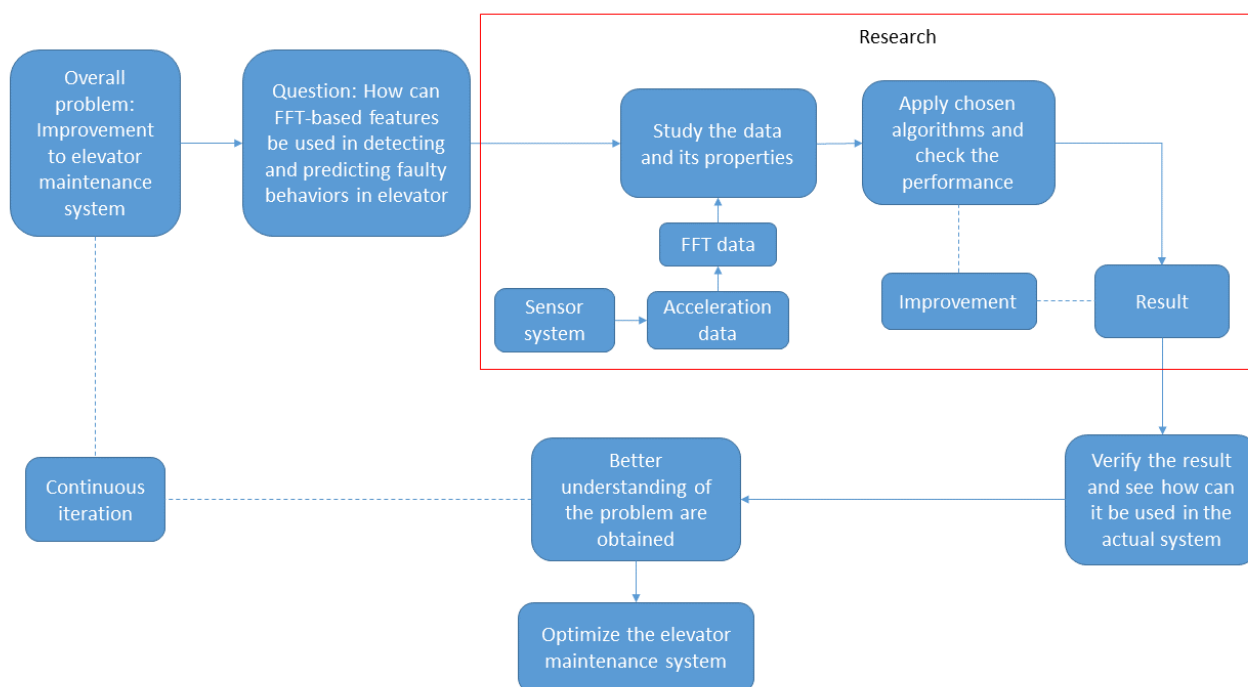
Figure 2. *A common approach toward solving the presented problem.*

This thesis consists of five chapters. The next chapter will present an overall theoretical background on the concepts and methods that are used in this work. It provides the introduction and mathematical explanation to the family of Fourier analysis in general and FFT in particular. After which, the detection of anomaly and methods of analyzing FFT data are

described. Chapter 3 will be about the data that are used in this work. It explains how the raw data is collected and how FFT is applied on it to obtain the FFT-based features or FFT data. The next part of the chapter is about the implementation of data analyzing models. Chapter 4 contains the criteria for evaluation, results obtained and discussion. Finally, Chapter 5 briefly summarizes the work and gives the conclusions. It also contains potential future improvements and ideas to expand on the topic.

2. THEORETICAL BACKGROUND

2.1 Fourier analysis

Fourier analysis is a method of representing or approximating signal as the sum of properly selected sinusoidal waves [11]. It is named after the French mathematician and physicist **Jean Baptiste Joseph Fourier** (1768-1830). Today, it has been used in numerous scientific applications like physics, number theory, signal processing, image processing, etc. From the Fourier analysis family, Fourier series can be considered to be an introductory case and it will be discussed in the following section.

2.1.1 Fourier series

Functions can be represented by a base set of other components, for example, a power series:

$$f(x) = \sum_{n=0}^{\infty} a_n x^n .$$

(1)

If a function $f(x)$ is periodic, it can be expanded into an infinite sum of sines and cosines. This expansion is what we call a Fourier series. As the relationship between sine and cosine functions is completely orthogonal over $[-\pi, \pi]$, the Fourier series of a periodic function $f(x)$ can be given as follow:

$$f(x) = \frac{1}{2} a_0 + \sum_{n=1}^{\infty} a_n \cos(n x) + \sum_{n=1}^{\infty} b_n \sin(n x) \ ,$$

(2)

where $a_0 = \frac{1}{\pi} \int_{-\pi}^{\pi} f(x) \, dx$

$a_n = \frac{1}{\pi} \int_{-\pi}^{\pi} f(x) \cos(n x) \, dx \ , \ n = 1, 2, 3 \dots$

$b_n = \frac{1}{\pi} \int_{-\pi}^{\pi} f(x) \sin(n x) \, dx \ , \ n = 1, 2, 3 \dots$

Using Euler's formula, the Fourier series (2) can be rewritten in complex form as:

$$f(x) = \sum_{m=-\infty}^{\infty} c_m \, e^{imx} \ ,$$

(3)

where

$$c_m = c_m(f) = \begin{cases} \frac{a_m}{2} + \frac{b_m}{2i}, & m = 1, 2, \ldots \\ \frac{a_0}{2}, & m = 0 \\ \frac{a_{-m}}{2} - \frac{b_{-m}}{2i}, & m = -1, -2, \ldots \end{cases}$$

As a result, we can have

$$c_m(f) = \frac{1}{2\pi} \int_{-\pi}^{\pi} f(x)\, e^{-imx}\, dx, \quad m = 0, \pm 1, \pm 2, \ldots$$

(4)

Fourier series expansion is a very useful tool to break up a periodic function into a set of basic terms which can be easily plugged in, solved individually, and then recombined in order to obtain the solution to the original problem or at least an approximation to it [12].

2.1.2 Discrete Fourier Transform

Let $x(t)$ be a 2π-periodic continuous signal. From (3), $x(t)$ can be written as a Fourier series:

$$x(t) = \sum_{m=-\infty}^{\infty} c_m\, e^{imt}, \qquad t \in [-\pi, \pi],$$

(5)

where c_m are the Fourier coefficients of $x(t)$.

Now, let N be an even positive integer and $t_k = \frac{2\pi k}{N}$, $k = -\frac{N}{2}, \ldots, \frac{N}{2} - 1$

Then the response at t_k is

$$x(t_k) = \sum_{m=-\infty}^{\infty} c_m\, e^{i\frac{2\pi k m}{N}}.$$

(6)

Because $e^{i2\pi kl} = 1$ for integers k and i, (6) can be rewritten as:

$$\sum_{m=-\infty}^{\infty} c_m\, e^{i\frac{2\pi k}{N}(m-lN)} = \sum_{l=-\infty}^{\infty} \sum_{-\frac{N}{2} \leq m-lN \leq \frac{N}{2}-1} c_m\, e^{i\frac{2\pi k}{N}(m-lN)}$$

$$= \sum_{l=-\infty}^{\infty} \sum_{n=-\frac{N}{2}}^{\frac{N}{2}-1} c_{n+lN}\, e^{i\frac{2\pi k}{N}n} = \sum_{n=-\frac{N}{2}}^{\frac{N}{2}-1} e^{i\frac{2\pi k}{N}n} \sum_{l=-\infty}^{\infty} c_{n+lN} = \sum_{n=-\frac{N}{2}}^{\frac{N}{2}-1} e^{i\frac{2\pi k}{N}n} X_n,$$

(7)

where $X_n, n = -\frac{N}{2}, \ldots, \frac{N}{2} - 1$ is given by

$$X_n = \sum_{t=-\infty}^{\infty} c_{n+lN} \ .$$

(8)

Combining (6) and (7), we have

$$x_k = x(t_k) = \sum_{n=-\frac{N}{2}}^{\frac{N}{2}-1} X_n e^{i\frac{2\pi k}{N}n} \ .$$

(9)

Formula (9) can be seen as an Inverse Discrete Fourier Transform, which was obtained in the process of discretization a continuous periodic signal. By solving the above formula with respect to X_n for $n = -\frac{N}{2}, \ldots, \frac{N}{2} - 1$, we obtain

$$X_n = \frac{1}{N} \sum_{k=-\frac{N}{2}}^{\frac{N}{2}-1} x_k e^{-i\frac{2\pi k}{N}n} \ .$$

(10)

Formula (10) is what we call the Discrete Fourier Transform (DFT) [13] and when it comes to digital signal processing (DSP), it is one of the most powerful tools for finding the spectrum of a finite-duration signal. In fact, because it is impossible for digital computers to process information that is not *discrete* and *finite* in length, DFT is the only type of Fourier transform that can be utilized in DSP [11].

2.1.3 Fast Fourier Transform

During the 1800s, Carl Friedrich Gauss introduced an algorithm that can compute DFT at a significantly reduced time [14]. However, at that time, necessary tools with sufficient computing power were lacking so the algorithm was made unpractical. However, in 1965, the time of computer revolution, J. W. Cooley and John Tukey independently rediscovered and popularized the algorithm again [11]. It was then that it gained the recognition it deserves. The so-called "Cooley-Tukey algorithm" is now commonly referred to as the Fast Fourier Transformation (**FFT**), and it is the most widely used algorithm to calculate DFT efficiently, often lowering the computation time by a factor of *hundreds* [11].

FFT uses the divide-and-conquer paradigm. It operates by decomposing the set of data to be transformed (*N*-point time domain signal) into a series of smaller data sets (*N* time domain

signals). The N frequency spectra are then calculated correspondingly to these N time domain signals. Finally, the single frequency spectrum is formed through the process of synthesizing the N frequency spectra [11].

In this work, FFT was chosen as the algorithm to analyze the properties of collected acceleration data and from that, detecting the potential anomalies.

2.2   Anomaly detection

Anomaly detection is the identification of data sections that significantly differ from a normal or regular pattern. Generally, anomaly detection can be categorized into two types: outlier and change point detection.

- **Outliers** are the data points that are suddenly distant from the rest of the normal samples, as illustrated in Figure 3. They can also be referred to as "spikes".
- **Change points** are defined to be the points in data where abrupt variations happen, either due to external influences or internal systematic alterations [15], as seen from Figure 4. These changes often signify the transition between states [16].
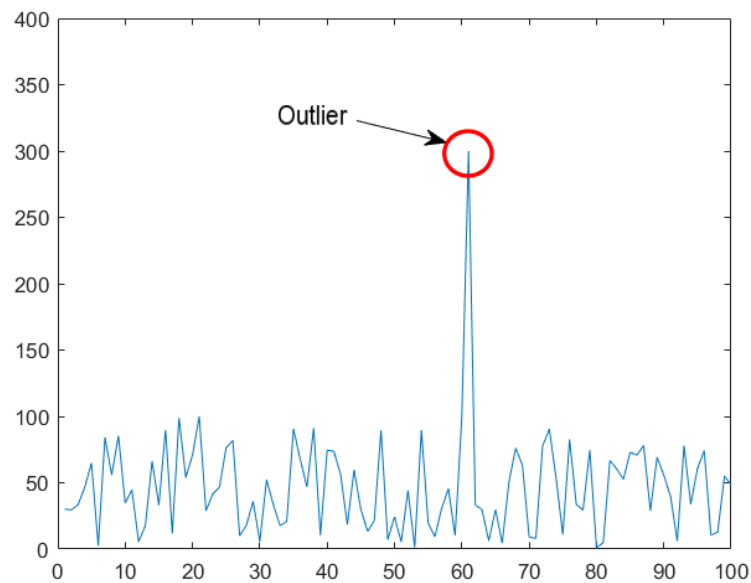
Figure 3. *An example of outlier in time-series data.*
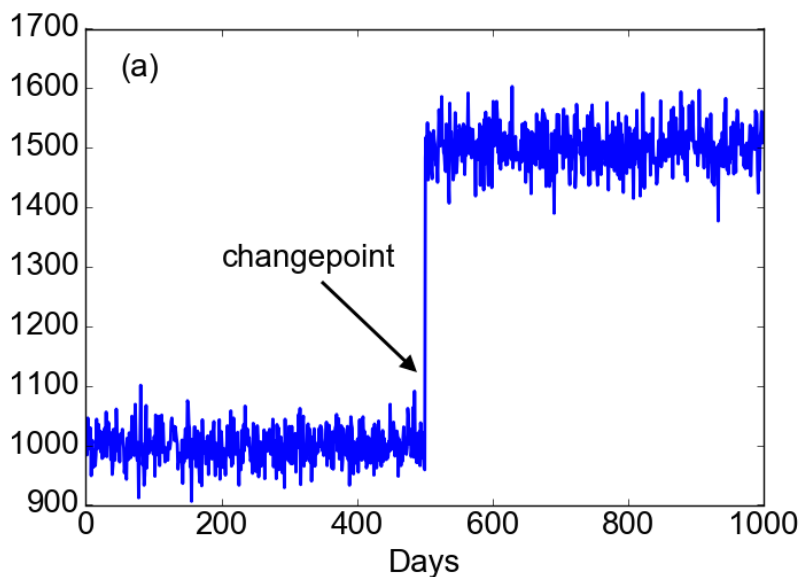
Figure 4. *An example of change point in time-series data.*

In elevator systems, an actual defective component will continue to display abnormal behavior until it is fixed or replaced. Therefore, it would be more beneficial to detect the change points where elevators started displaying these different behaviors, rather than detecting outliers, which might not necessarily be due to the bad condition of the equipment. Early detection of changes in elevator behavior can help the maintenance team find out potential abnormal elevators and take appropriate action if necessary. Thus, in this work, we decided to utilize change point detection in finding the possible faults in elevator systems. The detail of the change point detection algorithm will be described in Chapter 3.

2.3 Analyzing FFT data

Typically, FFT analysis for a machine like an elevator is used to monitor the condition of each piece of equipment in real time. The work is often done using analyzers and analysts are required to spend most of their time observing a stream of data and finding patterns as seen from an example in Figure 5. While being relatively effective, this method greatly relies on the individual skill and experience of the analyst and the cost can be considerably high. The problem becomes more and more serious as the population of elevators grows, and as a result, the need for an automated analyzing system using digital computers arises.
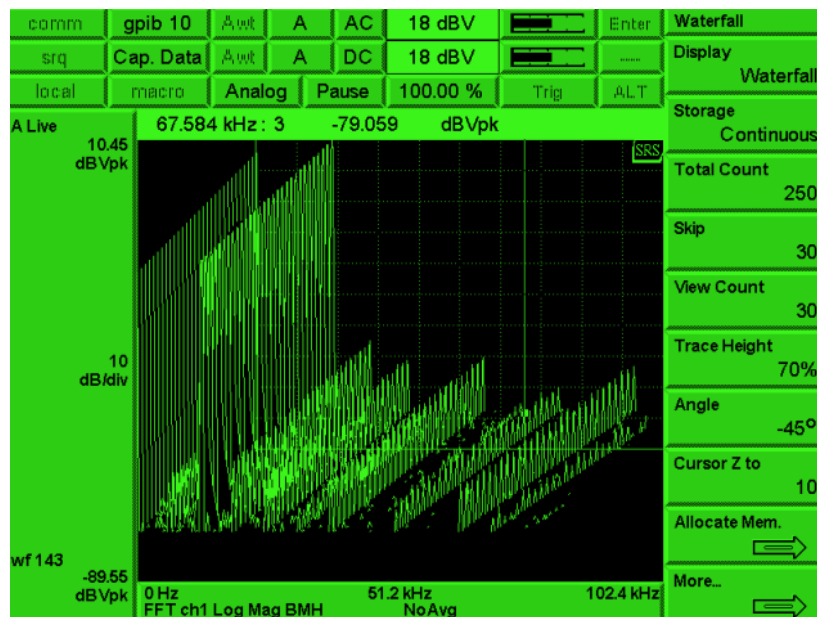
Figure 5. *An example of a FFT analyzer, model SRS785 [33].*

Data to be analyzed can often be classified into two groups:

- **Supervised data** which has both input and corresponding output variables (labels). The goal is to use learning algorithms to predict the outputs using given inputs, and then the predicted results can be compared with the given outputs to determine the accuracy of the algorithm.
- **Unsupervised data** which only has input variables and no corresponding output labels. The learning algorithms, in this case, can only learn the patterns of data and try to classify it without clear indicators for evaluation.

The goal of this work is to automatically detect the abnormality of elevators based on *unsupervised data*, where each FFT representation of a travel is considered to be a data point, depicted by a 1-by-511 vector. These data vectors together form a very high dimensional dataset, which makes analyzing become a challenging problem to tackle head-on [17]. The common practice is to analyze the data using only some of its most meaningful features and discard the redundant ones. In other words, it is to perform "dimensionality reduction".

There are two different approaches when it comes to dimensionality reduction, **feature selection** and **feature extraction**. The following sections are going to cover the definition of these two methods, as well as some of the more common techniques for each one.

2.4   Feature selection

Feature selection, also known as variable selection or attribute selection, is the process of selecting a subset consisting of most important features or variables from the original data to use in model construction [18]. By using feature selection, analysts can simplify models to

make them easier to interpret [19], shorten training, enhance generalization by reduction of variance/overfitting [19] [20] and finally, avoid the "curse of dimensionality" [17].

As mentioned previously, the central premise when using feature selection is that the data often contains some features that can be considered to be redundant or irrelevant and thus, it is possible to discard them without experiencing much loss of information [20]. This premise fits quite nicely with the data that is used in this work as in an FFT representation, oftentimes, some frequencies carry much more energy in comparison with the other frequencies in the observed spectrum. They are called the dominant frequencies [21] and for feature selection, an algorithm to detect these frequencies will be one of the main focuses in this work. Information about individual frequency and amplitude are retained in the process.

The implementation of this algorithm will be described in detail in Chapter 3.

2.5 Feature extraction

Similar to feature selection, feature extraction is also about reducing the dimension of the original data to a smaller set of features or variables, in order to make them easier to process and avoid the "curse of dimensionality". However, in contrast to feature selection, the new set of features is not a subset of the original data, but rather a set of completely new derived values. These new variables are obtained by transforming original data using different algorithms and are intended to capture their overall characteristics.

For FFT data, applying feature extraction will result in the loss of information about individual frequency and amplitude. However, feature extraction is expected to reliably capture the overall shape of the spectrum, and hence fulfill the general goal of accurately detect anomalies through amplitude changes within the data. Because of that, discarding those information should be acceptable if the overall objective is achieved through feature extraction.

There are several different algorithms that can be used for feature extraction. With regard to FFT data in rotating machines, the usage of feature extraction method like **Principal Component Analysis** (**PCA**) has been explored in recent research [22]. **Autoencoder**, a neural network based approach, has also been utilized when it comes to machine vibration analysis in general [23] [24]. In this work, the usage of Autoencoder on FFT data will be studied and experimented.

2.5.1 Feedforward Neural Network

An **Artificial Neural Network** (**ANN**) is an information processing paradigm inspired by the way biological nervous systems, most notably the brain, process information [25]. The key

component of this paradigm lies inside the novel structure of the system which comprised of a large amount of highly interconnected processing units (or neurons) working together to resolve a particular problem [25].

A **Feedforward Neural Network** (**FFNN**) is the simplest form of ANN, where connections between units, or neurons, do not form a directed cycle [26]. In this part, we are going to discuss the widely known model named **Multilayer perceptron** (**MLP**).

An MLP is a fully connected FFNN model with one or many hidden layers between input and output. These layers serve as computational neurons for the model. Figure 6 presents the basic form of an MLP with one hidden layer and one input. Multi-layer networks utilize a variety of learning methods, with the most common being back-propagation [27].

Suppose we have an input vector X with m-number of input units. The input will then be connected to a hidden layer, denoted by vector Y with n-number of neurons, using a combination of a non-linear activation function f_θ and a weight matrix $W^{(1)}$:

$$Y = f_\theta \left(X \times W^{(1)} + b^{(1)} \right),$$

where $b^{(1)}$ is the bias for the hidden layer.
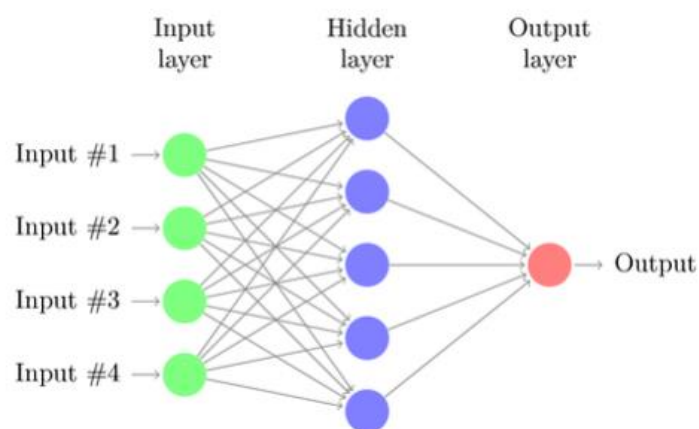
Figure 6. *MLP model of FFNN with one hidden layer and one input.*

The following layers are then computed in a similar manner until the output layer is reached. Via back-propagation, here, the outputs are compared with the given value to calculate a predefined error-function. Through various techniques, the error is then fed back to the network. With this information, the algorithm tries to adjust the weights of every connection in order to reduce the value of the error function. The process is then repeated sufficiently often and after which, the network generally converges to a state where the error of the calculations is relatively small. In this case, one would say that the model has been properly "trained" and a set of optimized weights has been produced [26].

In a classification task, the newly acquired weights will then be applied to the test set to check the model's performance in terms of accuracy.

2.5.2 Autoencoder

Architecturally, Autoencoder is a feedforward neural network. However, it is set apart by a major difference, which is the output layer. This last layer of an Autoencoder has an equal number of units as the input layer, and instead of training to predict an outside target values Autoencoder will try to reconstruct its own inputs [28].

In Autoencoder, the entire procedure can be generalized into two phases, encoding and decoding. First, when encoding, an Autoencoder takes the input X and map it to the hidden layer using the same representation as MLP:

$$Y = f_\theta \left(X \times W^{(1)} + b^{(1)} \right),$$

where f_θ, $W^{(1)}$, $b^{(1)}$ are the same as in MLP.

If there is only one hidden layer (as in Figure 7), the resulting latent representation Y will then be mapped back to a "reconstructed" vector Z with:

$$Z = g_\theta \left(Y \times W^{(2)} + b^{(2)} \right),$$

where g_θ is a non-linear activation function,

$W^{(2)}, b^{(2)}$ are weight matrix and bias for the output layer respectively.
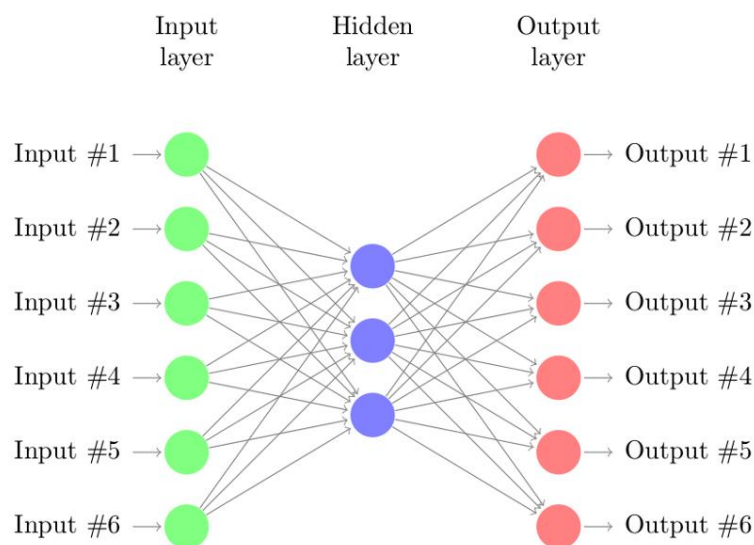
Figure 7. *Autoencoder model with one hidden layer.*

The network is then trained with back-propagation to minimize this reconstruction error. As this value shrinks, it is safe to assume that the hidden representation of the original input is a good representation. In other words, it must retain crucial information of the input in order to reconstruct as closely as possible. This is also considered to be the main purpose of Autoencoder, which is to compress data without losing its important or relevant features [28].

There are two commonly used variations of Autoencoder, Denoising Autoencoder and Sparse Autoencoder. Additionally, multiple hidden layers can also be stacked upon each other to create a Stacked Autoencoder or Deep Autoencoder. This practice oftentimes improves the ability to capture information in the hidden layer of Autoencoder. In this work, the model of Autoencoder that is used will be Stacked Sparse Autoencoder.

3. DATA DESCRIPTION AND IMPLEMENTATION OF ANALYZING METHODS

3.1 About the data

The data was collected from systems of sensor placed in elevators. For this work, accelerometers were used to measure the acceleration data from elevators in three dimensions, reflecting the mechanical vibrations of the elevator car during movement. Vertical acceleration data along the Z-axis, however, will be the main focus of this work as it generally presents a better visualization of events, especially in comparison with the other two horizontal axes (X and Y). The differences between data of these axes can be observed in an example from Figure 8.
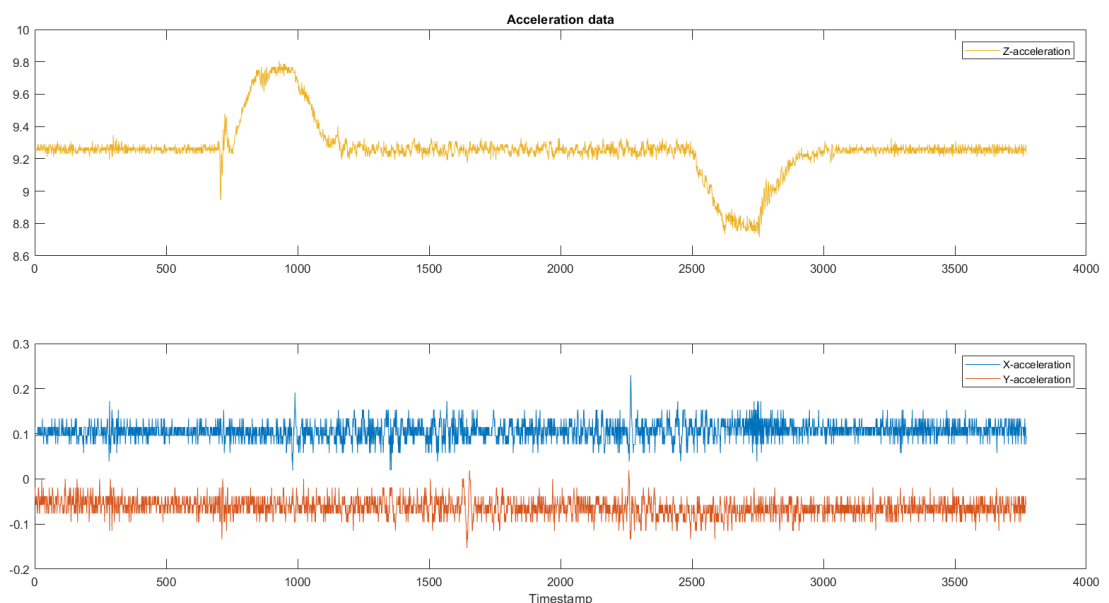
Figure 8. *Acceleration data from the X, Y and Z axes.*

Each instance of data corresponds to one travel, which is represented by one travel ID. A travel is defined as going from stationary → accelerating → constant speed → decelerating → stationary. For this work, only the constant speed phase is considered. This is because during the constant speed phase, the signal is more stable whereas during acceleration and deceleration, external influences from different machinery can interfere with the outcome when performing FFT.

For each travel, a 5-second window is selected in the middle, during the constant speed phase and FFT is applied to obtain the features. Consequently, if the length of the constant speed phase is less than 5 seconds, no FFT calculation is performed. The sampling rate of the accelerometer is 200Hz. Therefore, a 5-second window will contain 1000 samples and as a result, the FFT is calculated in 1024 frequency points (or bins).

Negative frequencies are discarded, along with the DC component (0Hz). In the end, 511 frequency points are retained and they are the 511 FFT-based features that are used in this work. Figure 9 presents detailed visualization on how the 5-second window is selected and the transformed region in frequency domain.
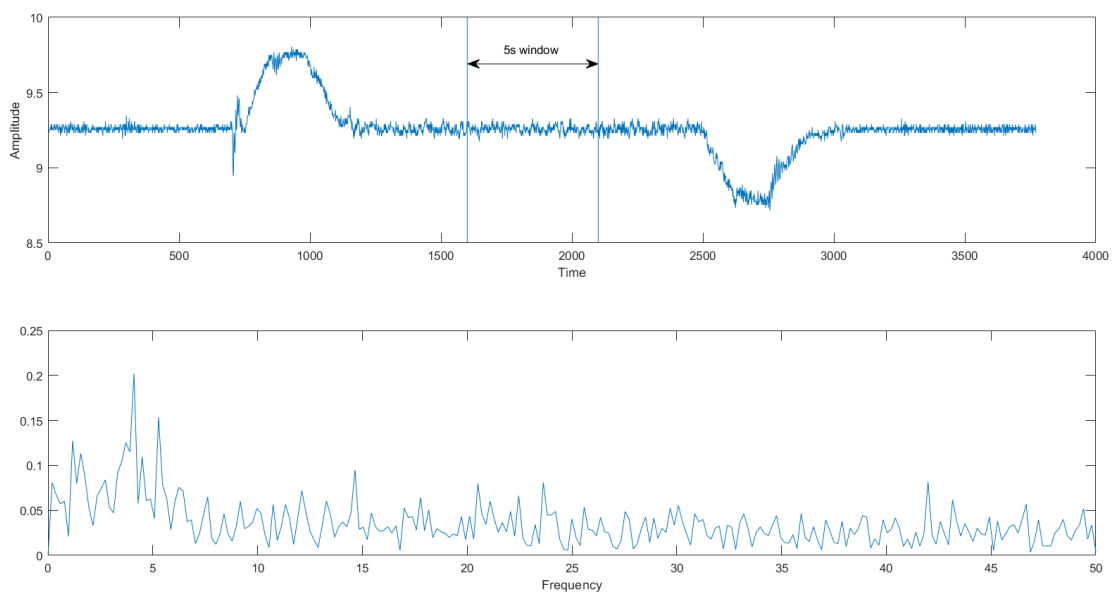
Figure 9. *Visualization of selecting window for FFT and frequency domain representation.*

It is worth noting that for elevators, upward and downward movements often have certain differences in characteristics. For that reason, they need to be investigated separately for each elevator.

The visualization of a sample elevator can be seen from Figures 10 and 11. Information about frequency, amplitude are presented, as well as the changing of data over a period of time. Differences between upward and downward movement can also be observed.
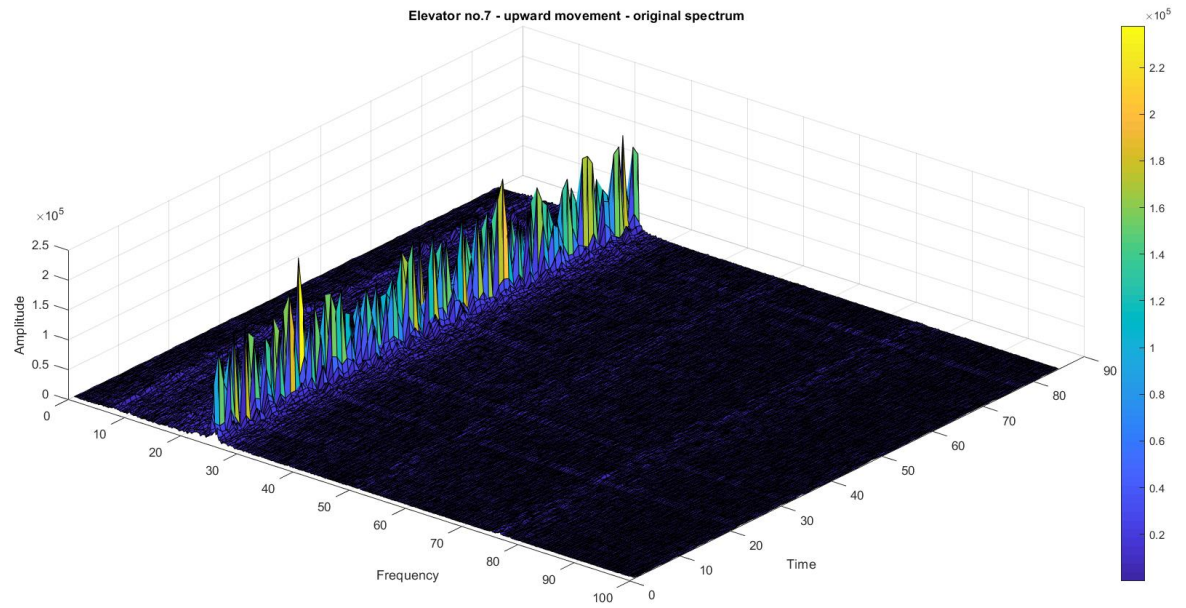
Figure 10. *Visualization of FFT data from elevator no. 7, upward movement.*
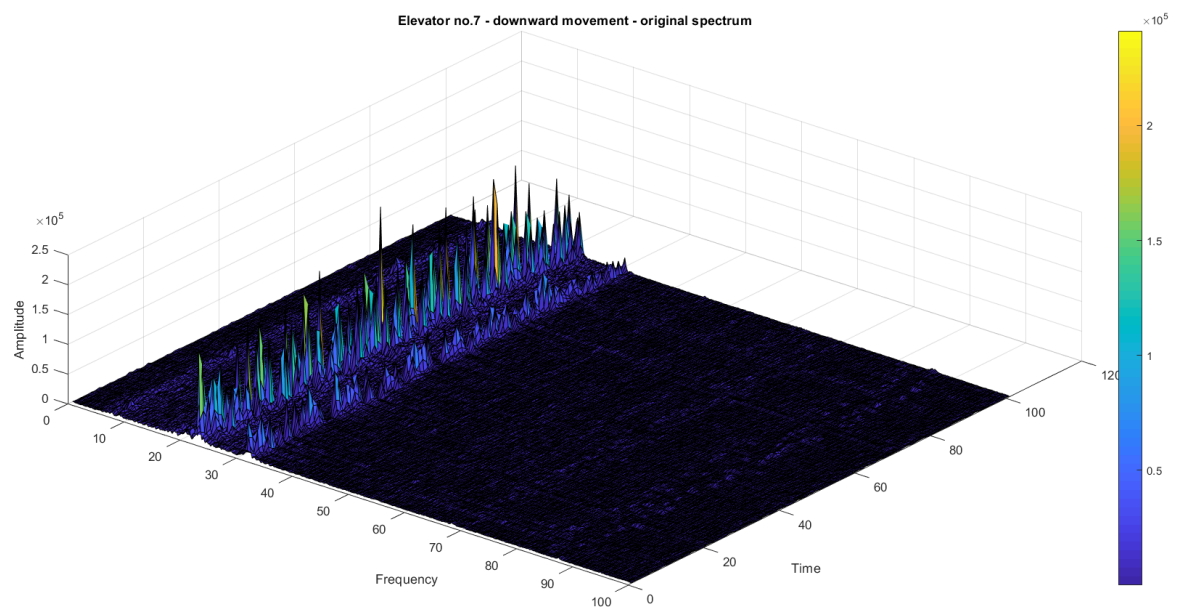
Figure 11. *Visualization of FFT data from elevator no. 7, downward movement.*

During the course of this work, a total number of 29 elevators were investigated, with each movement for each elevator contains from ~100 to 400 travels, and is represented by a dataset consisting of 511 columns.

3.2   Dominant frequencies analysis

In the FFT representation, one of the most important aspect to be analyzed is the dominant frequencies of the signal. Dominant frequencies are defined as the ones that carry the highest amount of energy among all frequencies presented in the spectrum [21]. Consequently, they are considered to be the main features and main focuses when analyzing the data. In order to find the most dominant frequencies for each movement of each elevator, we decided to create a method in MATLAB that detects energy peaks and the frequency ranges that they inhabit. The process is explained as follows

First, for each travel, the amplitude values are sorted in descending order and information about the frequency bins are kept. After that, the most dominant amplitudes are sorted again in descending order to find out the highest overall peaks of the data in each travel.

Next, the frequency that contains this amplitude, i.e., the most dominant frequency is selected. However, as can be observed from Figure 12, there is a phenomenon where the FFT bin that contains high energy varies slightly after each travel. Thus, it is necessary to consider not only the single dominant frequency bin, but also its neighbors as well. In this work, two more bins are added to both the left and the right, which makes up for a window of four is left out of the population.
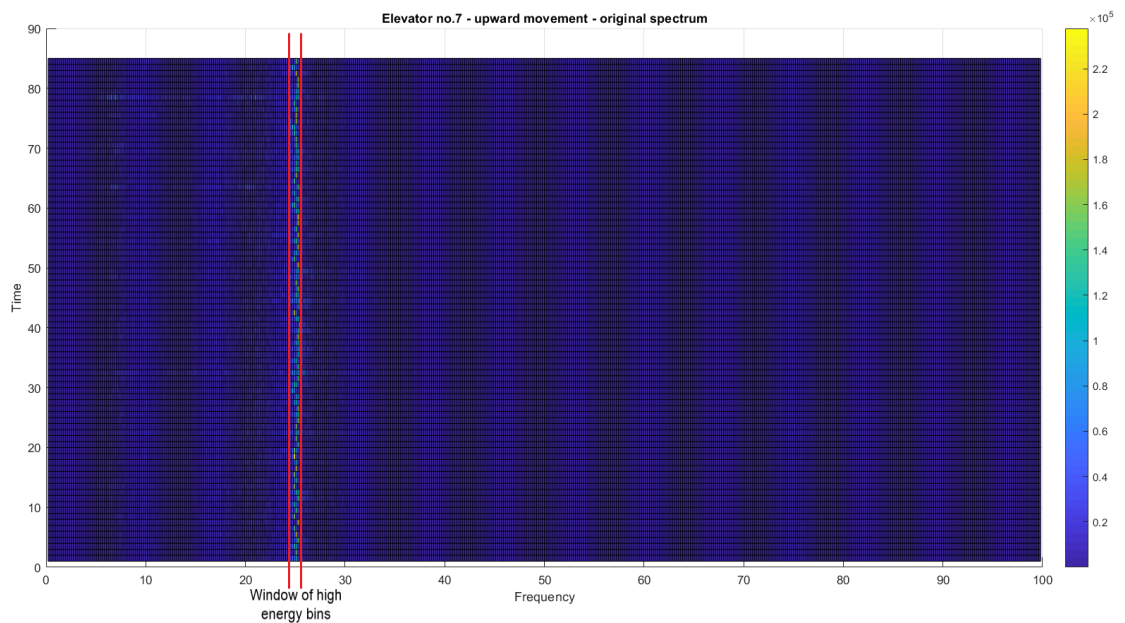
Figure 12. *Slight variation in high energy bin after each ride, elevator no. 7.*

The process is then repeated for at most two more subsequent dominant frequencies, resulting in three time-series vectors. A sample result of elevator no. 3 in Figure 10, upward movement can be seen from Figure 13 below.
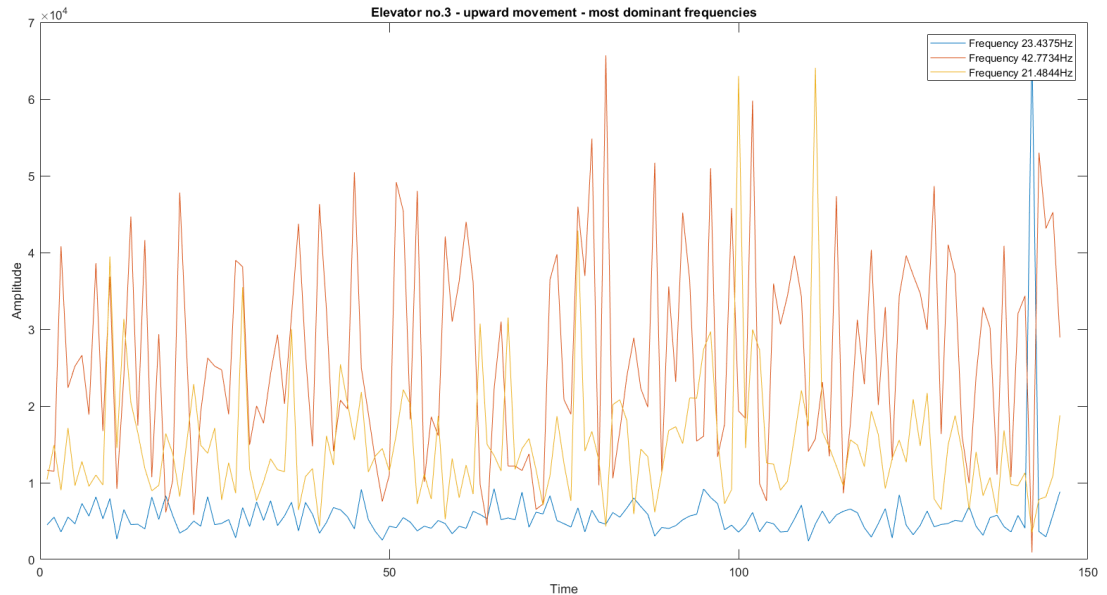
Figure 13. *Visualization of three frequencies that contain the highest energy peaks in elevator no. 3.*

Pseudocode:

```
Input: Dataset, Z
Output: Set of dominant frequencies, X and their amplitudes over time, Y
[Z_value, Z_index] = sort(Z, 2, 'descend'); // Sort elements in each row
of Z in descending order, keep the frequency indexes
max_Z = column 1 of Z_value; // Get the largest amplitude in each travel
(row)
max_Z_i = column 1 of Z_index; // Get corresponding indexes
sorted_pairs = sortrows([max_Z, max_Z_i], 'descend') // sort value-index
pairs by value, descending order
value_list = column 1 of sorted_pairs;
index_list = column 2 of sorted_pairs;
for i = 1 to length of index_list do
    if 3 dominant frequencies are found then break;
    if i is in already selected indexes then continue;
    else
            actual_index = index_list(i);
            select neighbors of  actual_index;
            select max values among neighbors as the amplitude values vector
of dominant frequency;
            add i and its neighbors to the pool of already selected indexes;
            add actual_index to X;
            add max values vector to Y;
    end
end
```

Program 1. *Pseudocode for dominant frequencies selection program.*

The change point detection will then be performed on the newly acquired set of vectors Y.

3.3   Autoencoder

By adding a regularizer to the cost function, we can encourage the sparsity of Autoencoder for the purpose of improving its ability to capture important information and learn richer representation [29], as well as prevent overfitting [30]. This regularizer is a function of the average output activation value of a neuron. The average output activation measure of a neuron i is defined as:

$$\widehat{\rho\iota} = \frac{1}{n}\sum_{j=1}^{n} z_i^{(1)}(x_j) = \frac{1}{n}\sum_{j=1}^{n} h\left(w_i^{(1)T}x_j + b_i^{(1)}\right),$$

where n is the total number of training examples,

   x_j is the j-th training sample,

   $w_i^{(1)T}$ is the i-th row of the weight matrix $W^{(1)}$,

   $b_i^{(1)}$ is the i-th entry of the bias vector $b^{(1)}$.

If a neuron has a high output activation value, it is considered to be "firing". Conversely, a low output activation value implies that the neuron in the hidden layer only "fires" in response to a small amount of the training samples. Having a lower value for $\widehat{\rho\iota}$ encourages the Autoencoder to learn a representation, where each hidden neuron responses to only a small number of training samples. In other words, each neuron focuses on responding to some features that are only presented in a small subset of the training data.

In this work, the Stacked Sparse Autoencoder model is implemented by training two Sparse Autoencoder model. The hidden layer of the first model consists of 128 hidden neurons and is trained for 400 maximum epochs, with the original 511-variable data as its input. The hidden layer is then used as the input for the second model. This contains a hidden layer with a size of 2 and is trained for 200 maximum epochs. In MATLAB, the model is visualized in Figure 14. The obtained hidden layer of the second model is the features extracted that will be used in detecting the changing point of data.
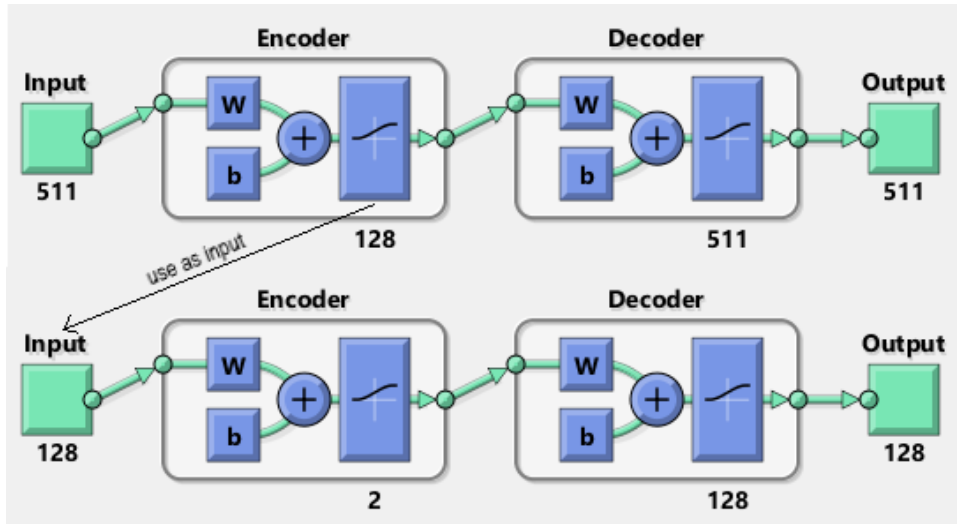
Figure 14. *Stacked Sparse Autoencoder in MATLAB.*

3.4 Change point detection

A change point of data can be detected by observing the change in its statistical properties, which can be for example mean, standard deviation, root-mean-square level or spectral characteristics. The function `findchangepts` from MATLAB is a ready-made tool to serve this purpose. This function uses a parametric global method, with the steps described as follows

- Divide the data into two sections by a *division point* chosen in advance.
- For each section, calculate the empirical estimate of the selected statistical property.
- At each point of the section, evaluate how much the property deviates from the empirical estimate and add that deviations for all points.
- Add the deviations section-by-section to determine the total error.
- Alter the position of the *division point* until the total error reaches a minimum [31].

For a given signal $x_1, x_2, \ldots, x_n$, the function tries to find k such that the total residual error

$$J(k) = \sum_{i=1}^{k-1} \Delta\big(x_i, \chi([x_1 \ldots x_{k-1}])\big) + \sum_{i=k}^{n} \Delta\big(x_i, \chi([x_k \ldots x_n])\big)$$

is the smallest.

If the observed statistical property is *standard deviation*

$$\sum_{i=a}^{b} \Delta\big(x_i, \chi([x_a \ldots x_b])\big) = (b - a + 1)\log \sum_{i=a}^{b} \sigma^2([x_a \ldots x_b])$$

$$= (b - a + 1)\log\left(\frac{1}{b-a+1}\sum_{i=a}^{b}\left(x_i - \frac{1}{b-a+1}\sum_{r=a}^{b} x_r\right)^2\right) = (b - a + 1)\log var([x_a \ldots x_b]).$$

If the observed statistical property is *mean*

$$\sum_{i=a}^{b} \Delta\left(x_i, \chi([x_a \ldots x_b])\right) = \sum_{i=a}^{b} (x_i - \mu([x_a \ldots x_b]))^2 = (b - a + 1)var([x_a \ldots x_b]),$$

where $var([x_a \ldots x_b])$ is the variance of vector $[x_a \ldots x_b]$.

In this work, at most 3 change points are to be detected by the algorithm.

4.   RESULTS AND DISCUSSION

4.1   Criteria for evaluation

As mentioned in the previous section, the data we analyzed is *unsupervised* and at the time of this study, the only way we could use to estimate the correctness of change point detection is through visualization. In short, we observed the FFT spectrum of each elevator and tried to detect the ones that contain clear visual changes. For cases that do contain changes, we can estimate the change points and take them as the *target outputs* for our algorithms. The idea is to see if our implementation of feature selection and feature extraction together with change point detection can correctly these target change points. Aside from accuracy, time is also a factor to be considered in order to determine which technique is more efficient.

After that, for each elevator, the data before and after the change point are inspected to see how much the change is in percentage. This change is calculated by comparing the amplitude mean of each data section. By doing this we can single out the most problematic elevators, which contain a high percentage change in vibration amplitude compared to others. This can be valuable for the maintenance team, especially when the number of monitored elevators is large and there needs to be a priority list. The percentage change algorithm will also ignore short windows of change with a length smaller than 10 elevator rides, which can be considered as artificial amplitude spike due to an external force, like people jumping inside elevators, and not an internal problem. The overall process is described in Figure 15.
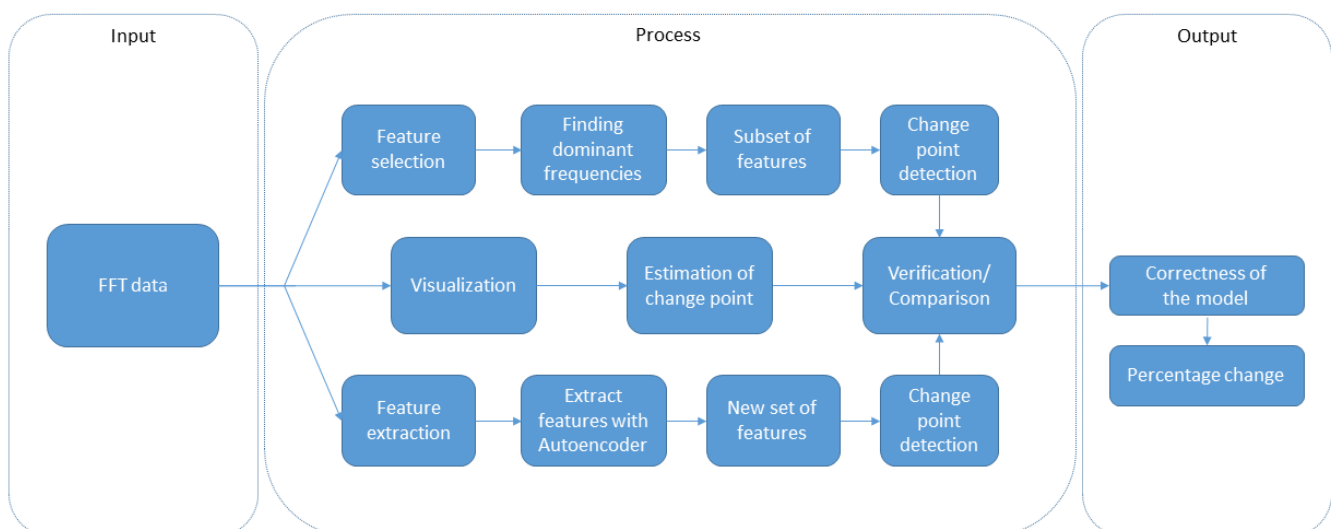
Figure 15. *Overall process flowchart.*

Expected results:

- **Cases with clear visual changes**: change points detected match the *target outputs*
- **Cases without clear visual changes**: small percentage change compared to cases that have clear visual changes

4.2 Results

In this section, four different elevators, each with different behavior, are presented and analyzed. The first one is elevator no. 1, which has no visible change in vibration amplitude. The second is elevator no. 14 with a noticeable but small change. Next is elevator no. 15 with both amplitude increase and decrease. The last one is elevator no. 21 with a large amplitude increase. For the first three elevators, only the results for upward movement are presented in the following section in visual form. As elevator no. 21 contains some interesting characteristics, both upward and downward movements of this device will be displayed. For the remaining cases, they can be found in the subsequence summary tables.

For each case, we first display its original spectrum. After that, if there is any change in vibration amplitude, markers will be placed to signify the visual change points or *target outputs*. The results from feature selection and feature extraction are presented next, together with change points detected in each method. The default statistical property for change point detection is *standard deviation* unless stated otherwise. Finally, for cases with noticeable changes in amplitude, we summarize the results by comparing them with the ones acquired from visual detection in a single figure.

4.2.1 Elevator no. 1, upward movement

Figure 16 shows the original spectrum of FFT data from elevator no. 1, upward movement. As can be seen from the figure, the vibration amplitude level remains quite stable for the whole spectrum. This is an example of cases where elevators display no noticeable change in vibration amplitude.
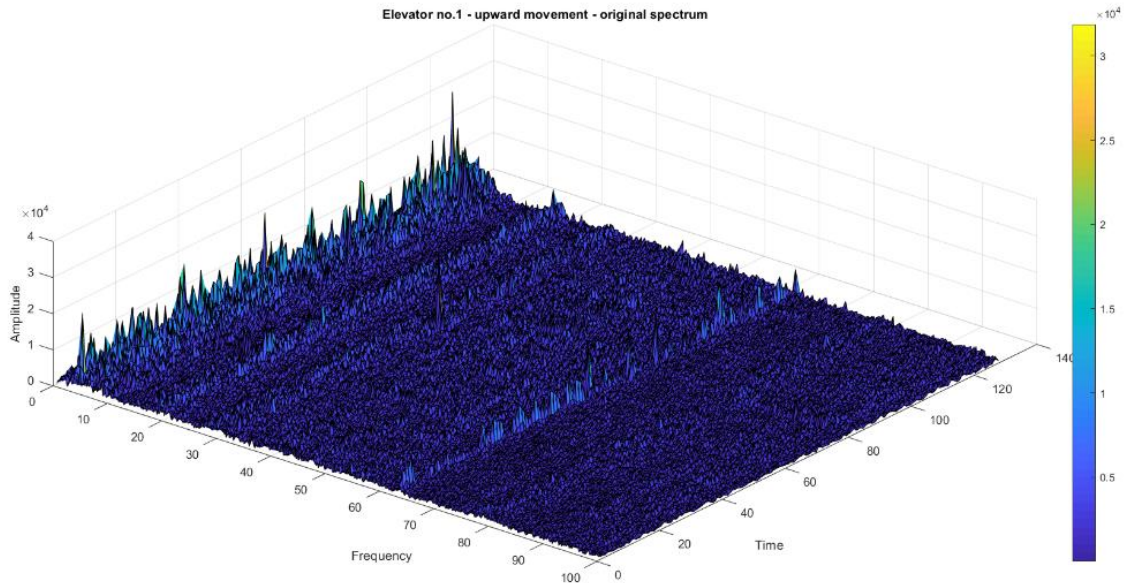
Figure 16. *Original spectrum of elevator no. 1, upward movement.*

Three most dominant frequencies of elevator no. 1, upward movement are selected using feature selection. Change point detection is then applied to find out if the vibration amplitude level is really stable or not. The results are displayed in Figure 17.
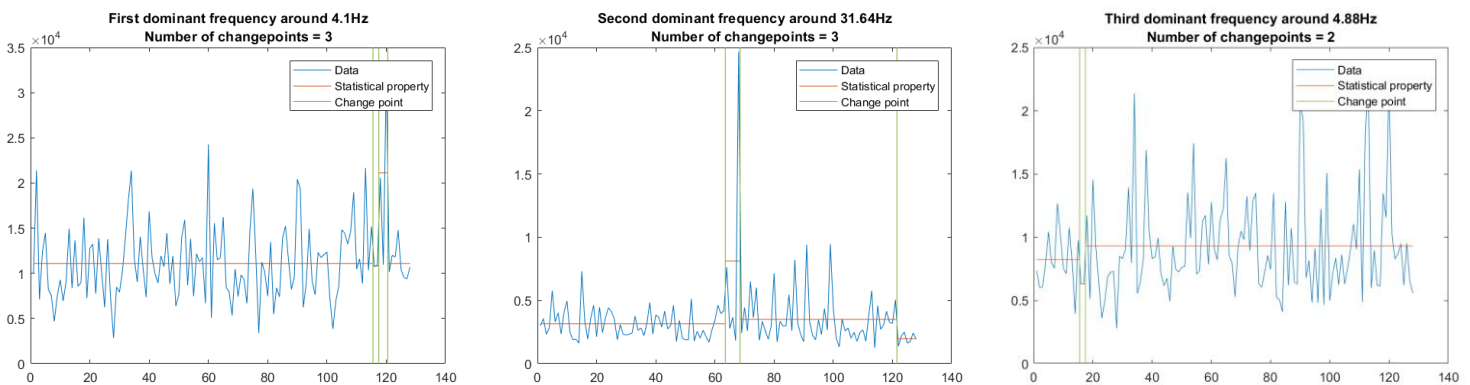
Figure 17. *Results for change point detection of three most dominant frequencies of elevator no. 1, upward movement.*

From the results in Figure 17, we can see that in all three frequencies, some changes were detected. However, the changes in frequencies 4.1Hz and 31.64Hz are due to the single spikes, and the vibration amplitude went back to normal immediately afterward. For the case of 4.88Hz, the amplitude increased by a marginal percentage of 14.70% in mean. The total calculation time of feature selection was 0.25 seconds.

Using Autoencoder on the data of elevator no. 1, upward movement, we can acquire the extracted features that represent the shape of the spectrum. Figure 18 shows the two features together with the change point detection results.
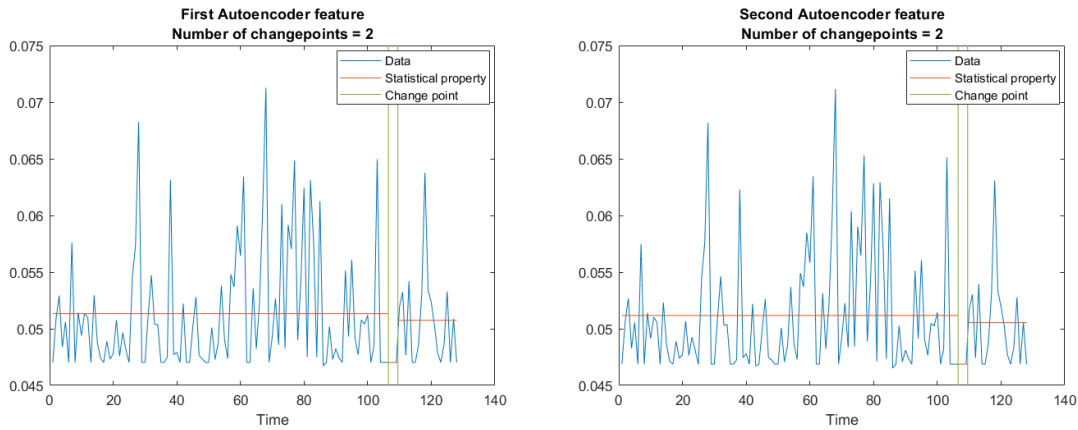
Figure 18. *Results for change point detection of two extracted features of elevator no. 1, upward movement.*

As can be seen from Figure 18, even though changes were detected, the overall statistical value stayed largely the same. The total calculation time of feature extraction was 13.84 seconds.

All in all, for upward movement of elevator no. 1, both algorithms succeed in determining that there were no significant or visible changes in vibration amplitude. Feature selection, however, is significantly faster than feature extraction.

4.2.2 Elevator no. 14, upward movement

The original spectrum of elevator no. 14, upward movement can be seen from Figure 14. We can easily notice a slight change in vibration amplitude at around 50-55Hz.
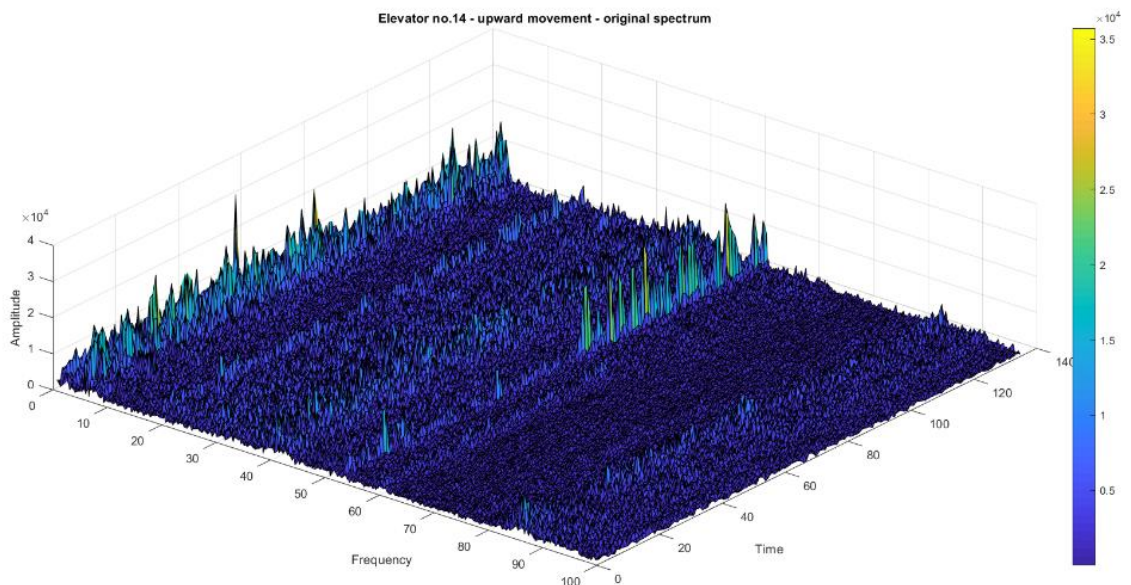
Figure 19. *Original spectrum of elevator no. 14, upward movement.*

By looking at the spectrum from another angle, we can clearly see the point where overall vibration amplitude changes. This can be seen from Figure 20.
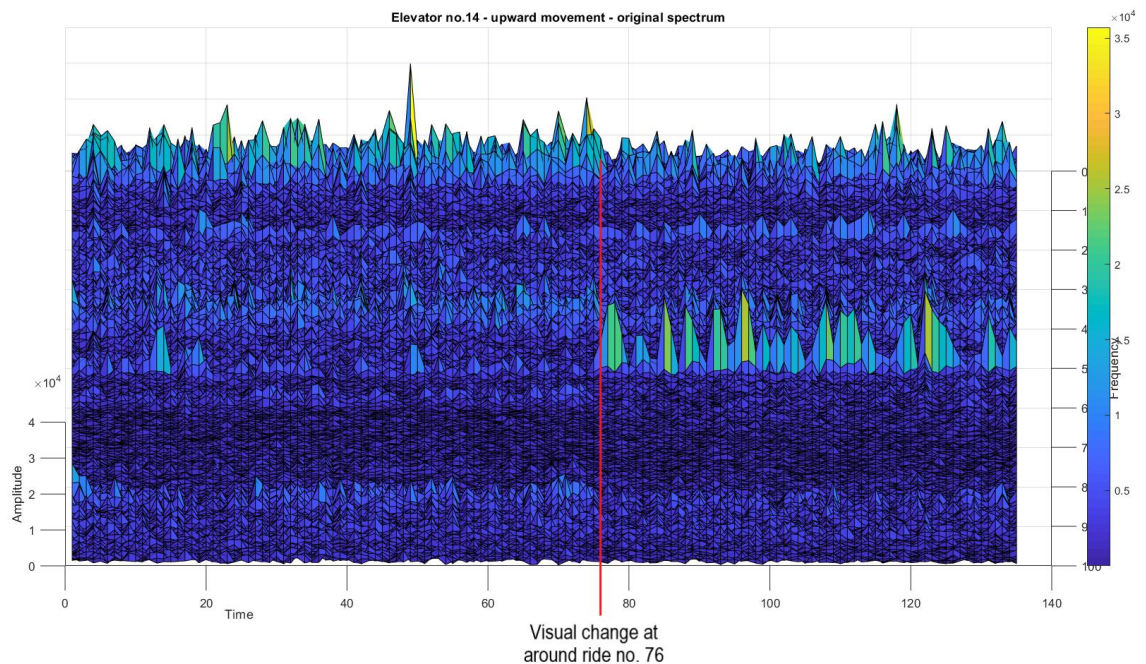
Figure 20. *Visually detected change point for elevator no. 14, upward movement.*

Using feature selection, we can find out the three most dominant frequencies from elevator no 14, upward movement. These frequencies, as well as their respective change points detected are shown in Figure 21.
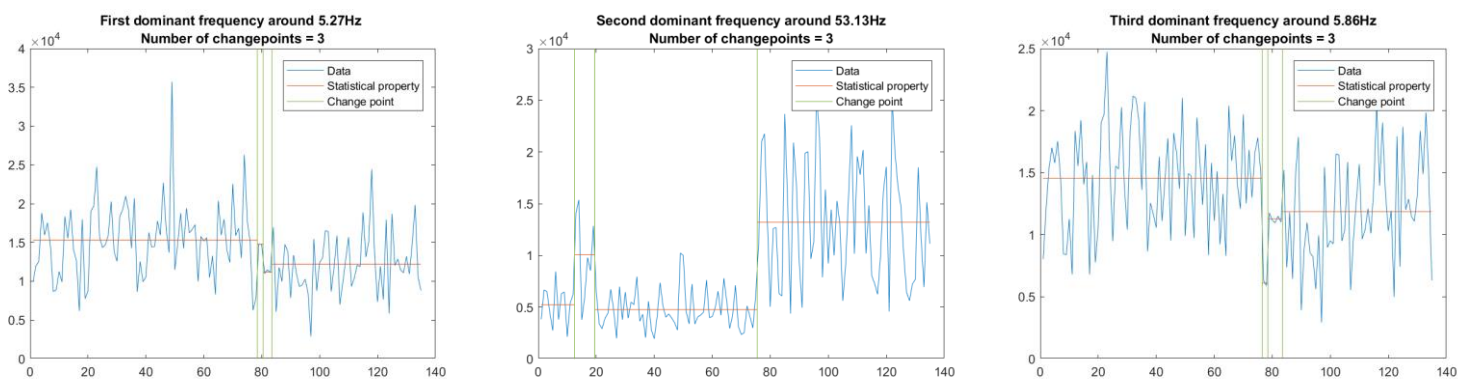
Figure 21. *Results for change point detection of three most dominant frequencies of elevator no. 14, upward movement.*

As can be observed from the results in Figure 21, the algorithm has successfully detected the change point at around ride no. 76 for frequency 53.13Hz. We can see a clear amplitude increase in amplitude (170.96%), which is also visible in the original spectrum. For the other two frequencies, 5.27Hz and 5.86Hz, the change points were detected at ride no. 79 and no. 77 respectively, and the amplitude actually went down slightly afterward. In this case, the calculation time was 0.23 seconds.

Figure 22 shows the extracted features of elevator no. 14, upward movement data, as well as their change points detected.

Figure 22.   *Results for change point detection of two extracted features of elevator no. 14, upward movement.*

From Figure 22, we can see that for Autoencoder, the change point at around ride no. 76 was also correctly identified for both features. Calculation time in this case was 13.42 seconds.

A comparison of results can be found in Figure 23. In this figure, the change points shown are the closest to the visual marking from Figure 20.
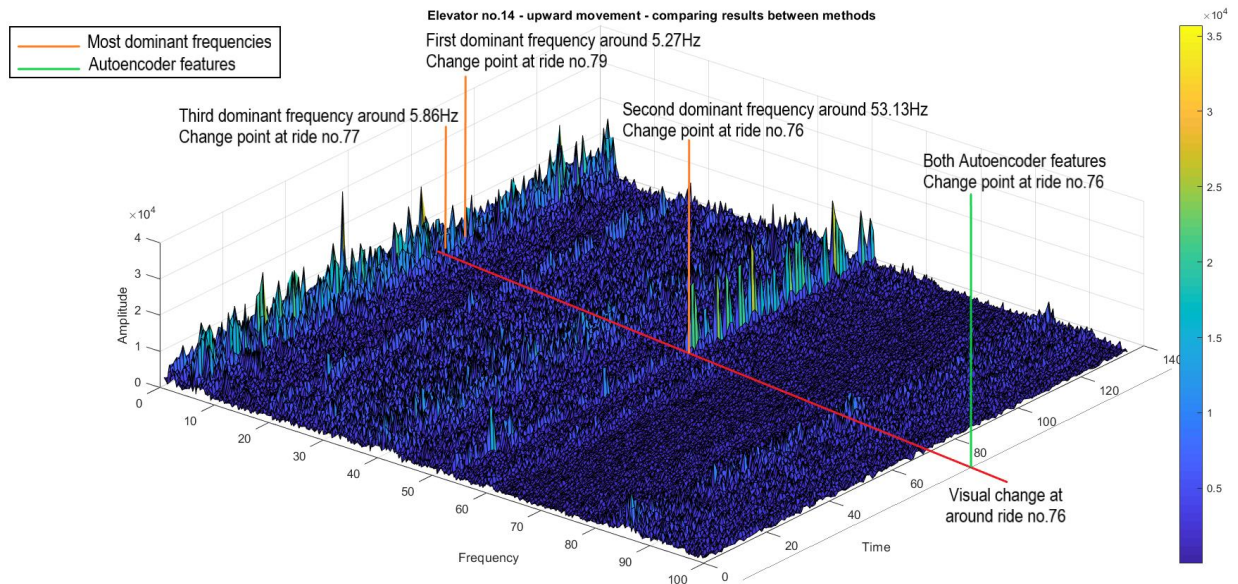
Figure 23.   *Comparison of change points detected for elevator no. 14, upward movement.*

With the case of elevator no. 14, for upward movement, both algorithms have successfully identified the visible change point at around ride no. 76. Change point detection also detected

other changes but they can be considered to be noise. Feature selection is once again faster than feature extraction when considering the time factor.

4.2.3 Elevator no. 15, upward movement

Figure 24 shows the original spectrum of elevator no. 15, upward movement. For this case, we can see that there are two major points where the vibration amplitude level changes. The first change point is when the amplitude level increases while the second one is when the level goes back to normal.
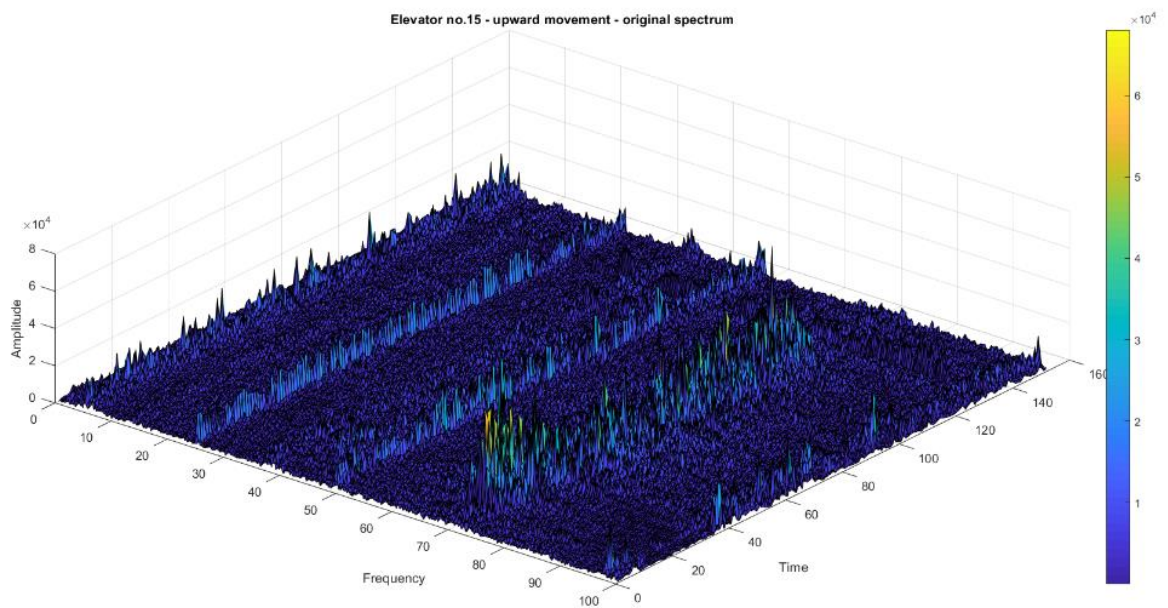
Figure 24.   *Original spectrum of elevator no. 15, upward movement.*

Similar to elevator no. 14, we can rotate and see the spectrum from another angle. This can be seen from Figure 25. Two visual cues have also been placed to mark the change points, which are around ride no. 12 and ride no. 120.
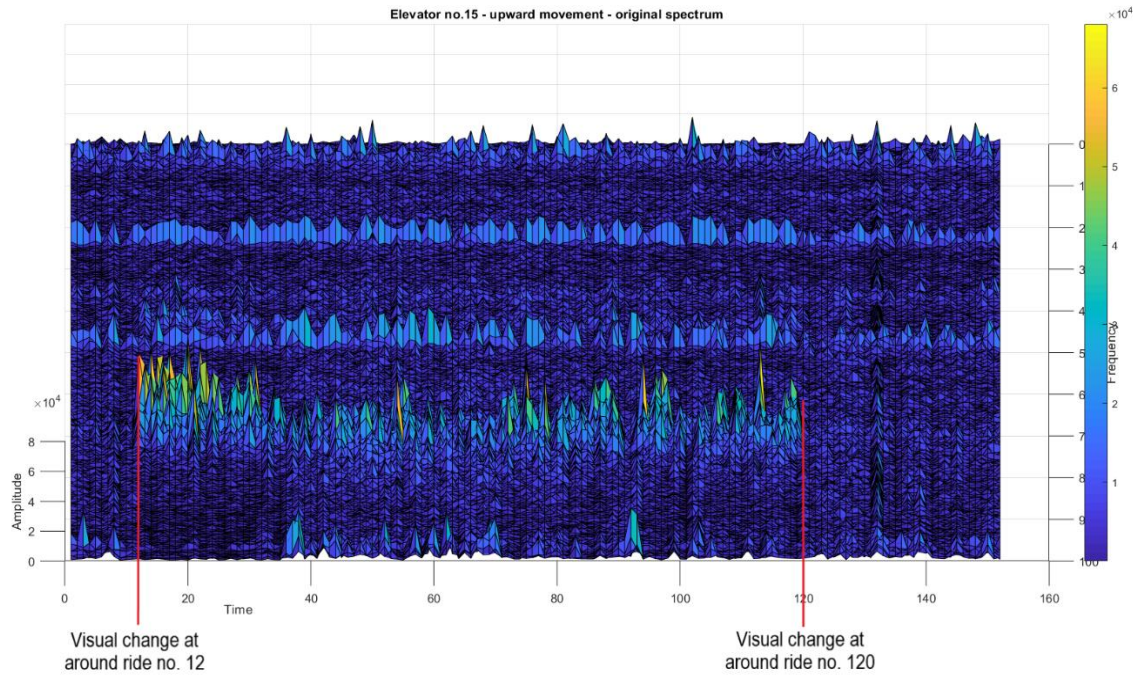
Figure 25. *Visually detected change points for elevator no. 15, upward movement.*

Figure 26 shows the most dominant frequencies in the spectrum of elevator no. 15, upward movement. The results from change point detection are also presented for each frequency.
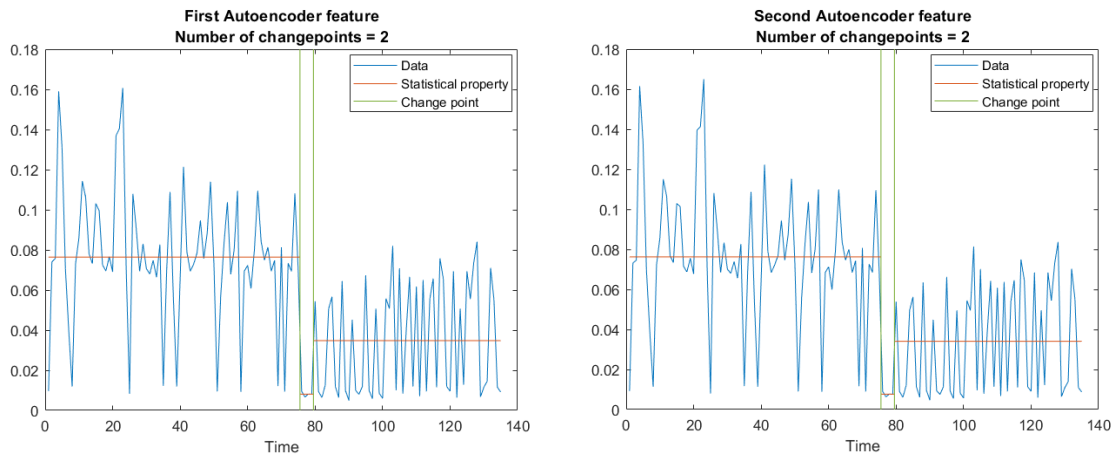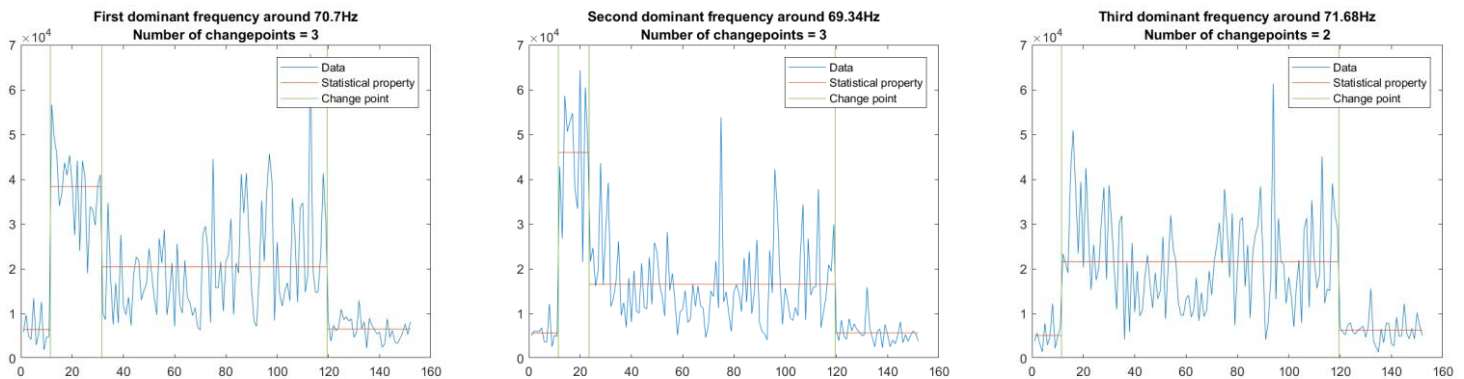

Figure 26. *Result for change point detection of three most dominant frequencies of elevator no. 15, upward movement.*

As can be seen from the three results in Figure 26, the major change points at around ride no. 12 and ride no. 120 were detected successfully. The percentage increase were 247.78% for the first frequency, 403.26% for the second one and 222.34% for the third. As the increase in vibration amplitude might indicate a problem within the elevator, the decrease at around ride no. 120 could mean that this problem has been fixed by the maintenance team. Total calculation time, in this case, was 0.25 seconds.

The features extracted by Autoencoder for elevator no. 15, upward movement and their change points are displayed in Figure 27. Some differences compared to previous elevators can be noticed in this case.
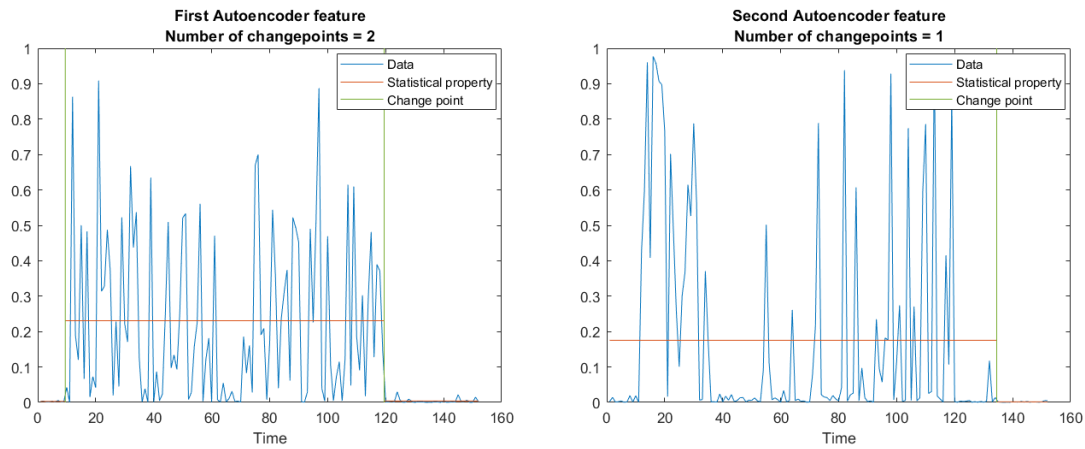
Figure 27. *Result for change point detection of two extracted features (standard deviation) of elevator no. 15, upward movement.*

Through visual inspection of Figure 27, we can easily detect the obvious change points at around ride no. 12 and ride no. 120. However, the change point detection algorithm, using the difference in standard deviation, only managed to spot these points for the first extracted feature and failed for the second one.

In order to successfully detect the change points at ride around no. 12 and no. 120 in the second extracted feature, the statistical property needs to be changed from *standard deviation* to *mean* and the *number of maximum change points* needs to be 5. Calculation time, in this case, was 14.36 seconds.

By performing change point detection again, this time with updated parameters, we can acquire the results shown in Figure 28. The change points have now been correctly detected.
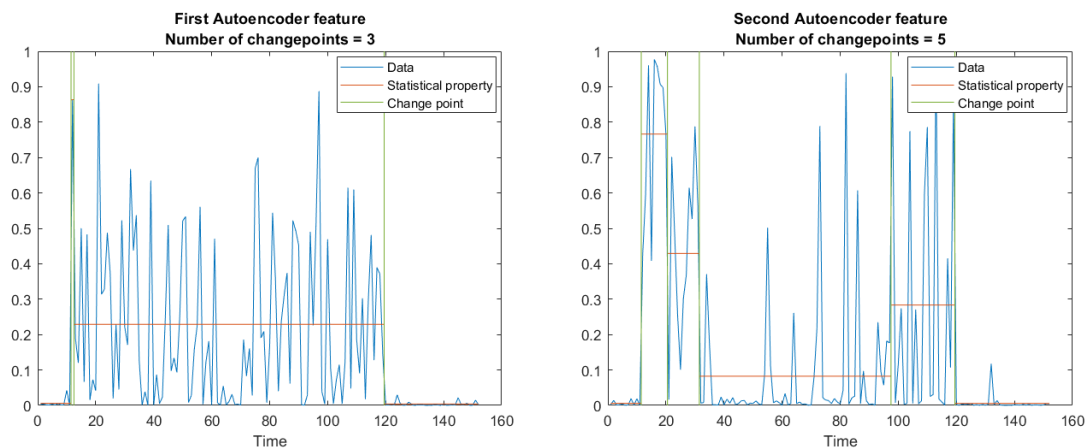
Figure 28. *Result for change point detection of two extracted features (mean and maximum 5 change points) of elevator no. 15, upward movement.*

Overall, for elevator no. 15 going upward, feature selection and change point detection were able to accurately detect the 2 major changes at around ride no. 12 and no. 120. For feature extraction, even though the extracted features provided a good representation of original data, change point detection was unable to detect the change for the second feature without modifying the parameters. Once again, time calculation is significantly lower for feature selection.

Figure 29 compares the detected change points from feature selection and feature extraction against the change acquired through visual detection. For feature extraction, results from change point detection with updated parameters are shown.
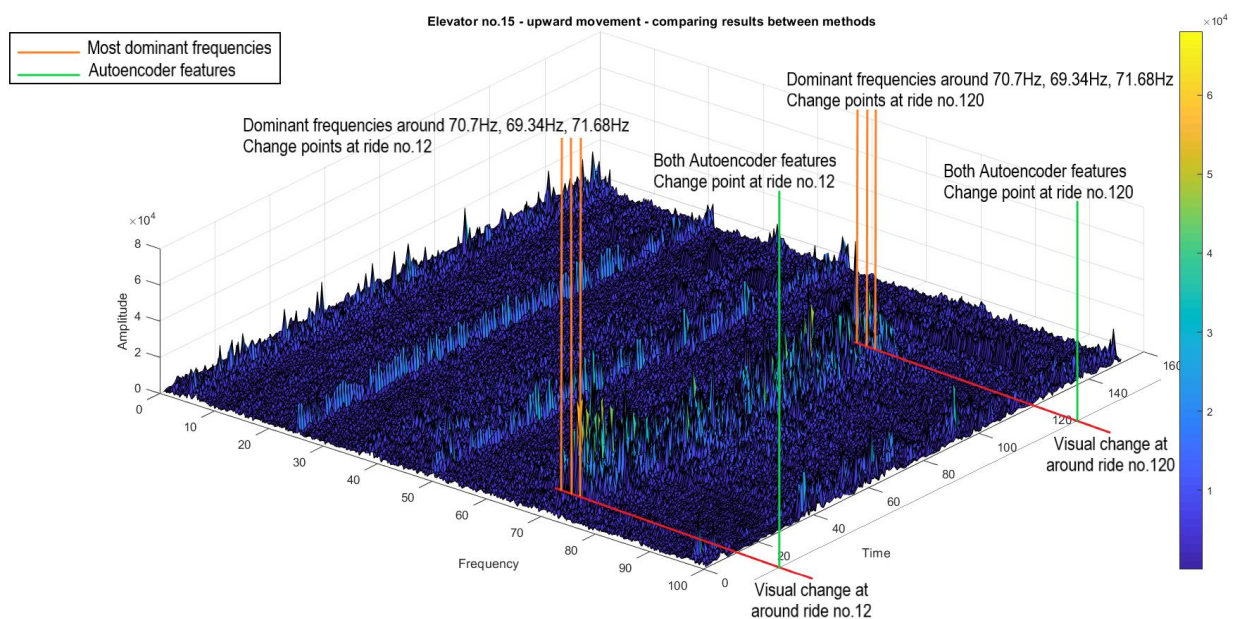
Figure 29. *Comparison of change points detected for elevator no. 15, upward movement.*

4.2.4 Elevator no. 21, upward movement

The original spectrum of elevator no. 21, upward movement is shown in Figure 30. Here we can see a very significant change in vibration amplitude level toward the end of the spectrum.
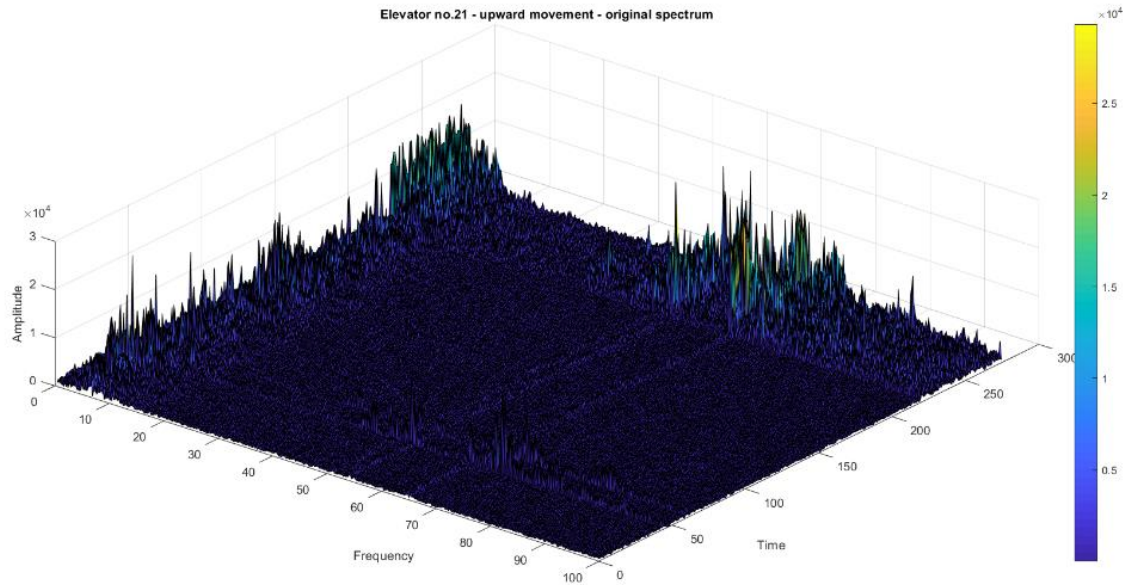
Figure 30. *Original spectrum of elevator no. 21, upward movement.*

Figure 31 shows the spectrum from another angle, as well as a marking for the change point detected through visual inspection.

Figure 31. *Visually detected change point for elevator no. 21, upward movement.*

Selected features, or dominant frequencies of elevator no. 21, upward movement are displayed in Figure 32. The change point detected can also be observed from the figure.
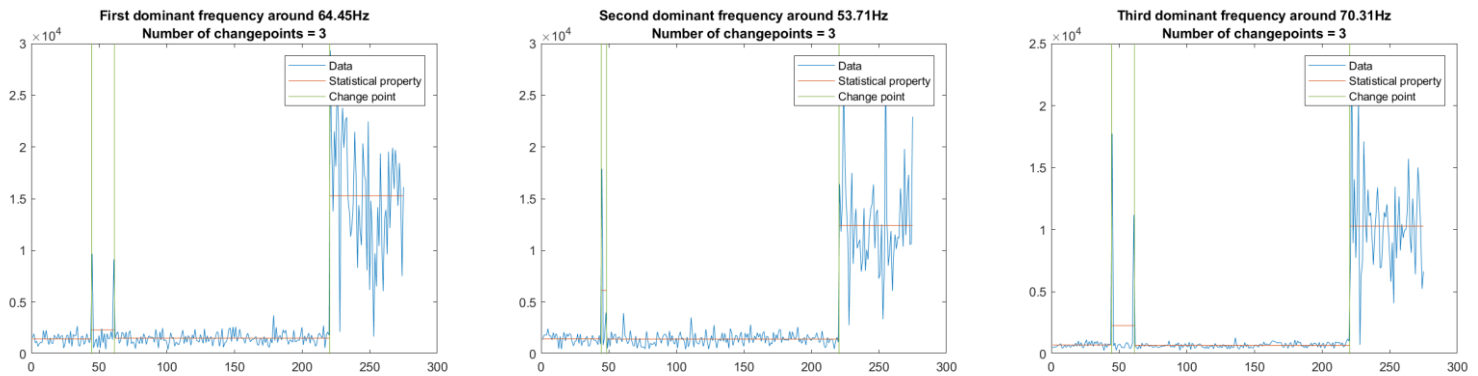
Figure 32. *Result for change point detection of three most dominant frequencies of elevator no. 21, upward movement.*

As can be seen from the results in Figure 32, the major change at around ride no. 221 was properly identified in all three dominant frequencies. The percentage increase in mean amplitude are very high, 805.74% for the first frequency (64.45Hz), 716.61% for the second (53.71Hz) and 1305.32% for the third (70.31Hz). The calculation time, in this case, was 0.26 seconds.

For Autoencoder, the extracted features as well as their respective change point detected can be found in Figure 33.
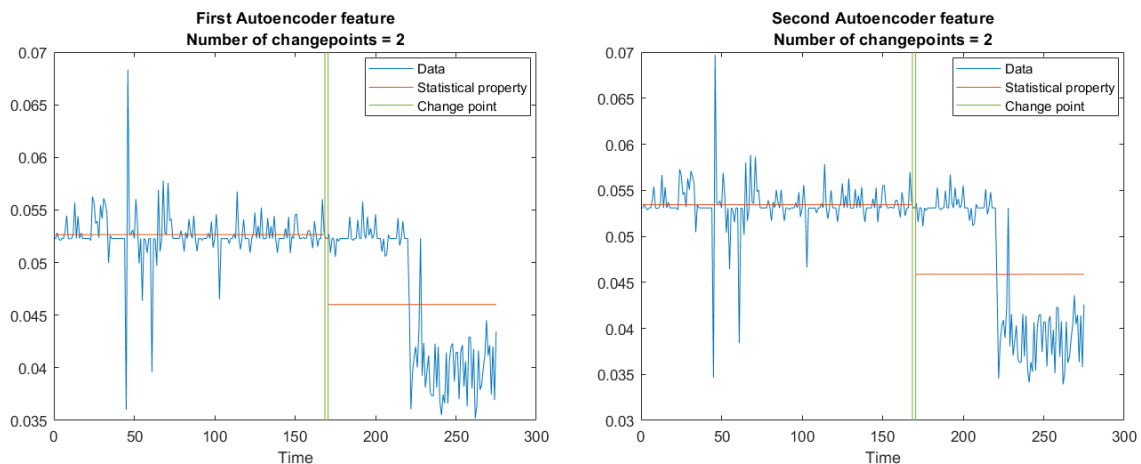
Figure 33. *Result for change point detection of two extracted features (standard deviation) of elevator no. 21, upward movement.*

From the results in Figure 33, we can easily notice the change point at around ride no. 221. However, similar to elevator no. 15, change point detection did not manage to detect the correct change when the statistical property is *standard deviation*. If this is changed to mean, the results are different.

Figure 34 shows the new results when applying change point detection again, this time with *mean* as the statistical property.
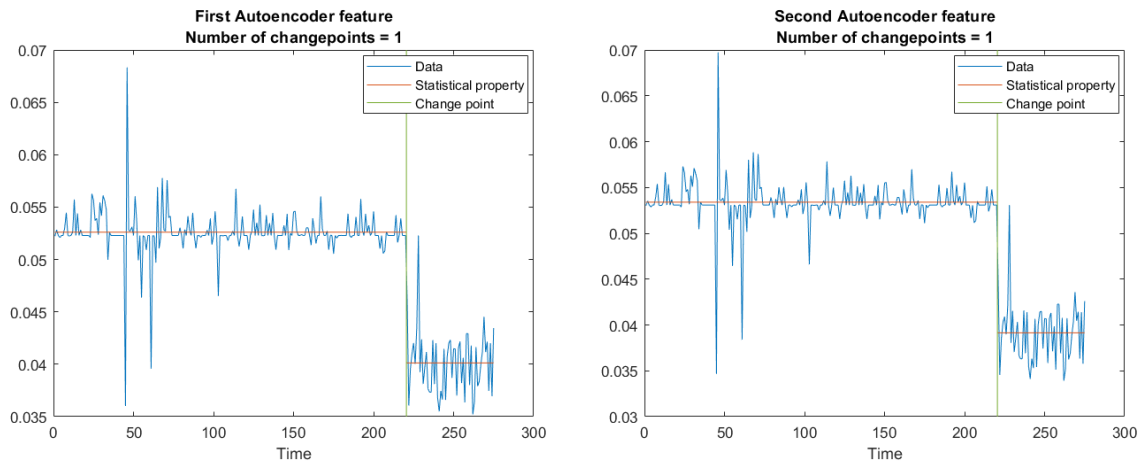
Figure 34.   *Result for change point detection of two extracted features (mean) of elevator no. 21, upward movement.*

The change point has now been corrected detected for each extracted feature. The calculation time, in this case, was 17.26 seconds.

The detected change points from two techniques are compared with the one from visual detection in Figure 35. Similar to elevator no. 15, results for Autoencoder are from change point detection with modified parameters.
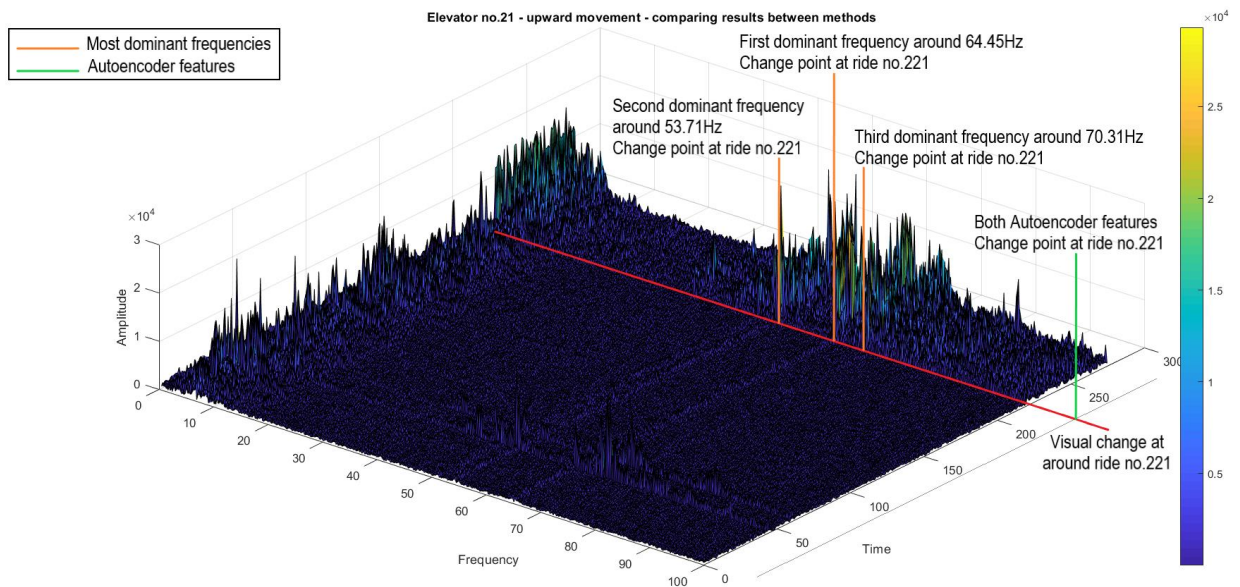

Figure 35.   *Comparison of change points detected for elevator no. 21, upward movement.*
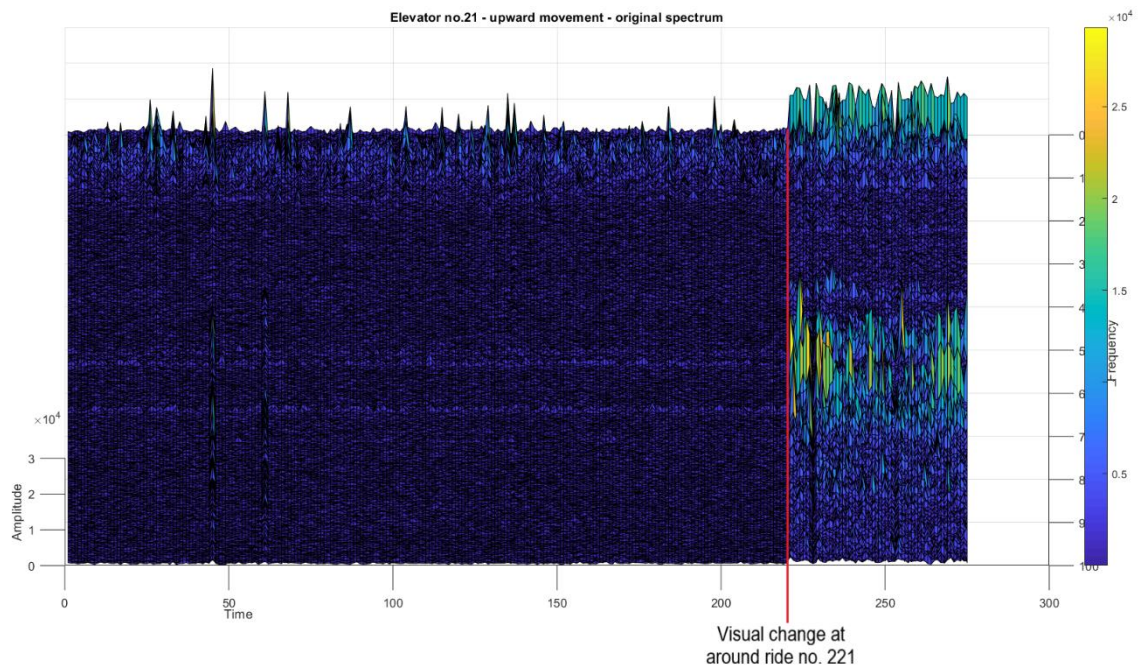
4.2.5 Elevator no. 21, downward movement

Figure 36 shows the original spectrum of elevator no. 21, downward movement. Similar to the upward case, we can see a clear change in vibration amplitude level near the end of the spectrum.
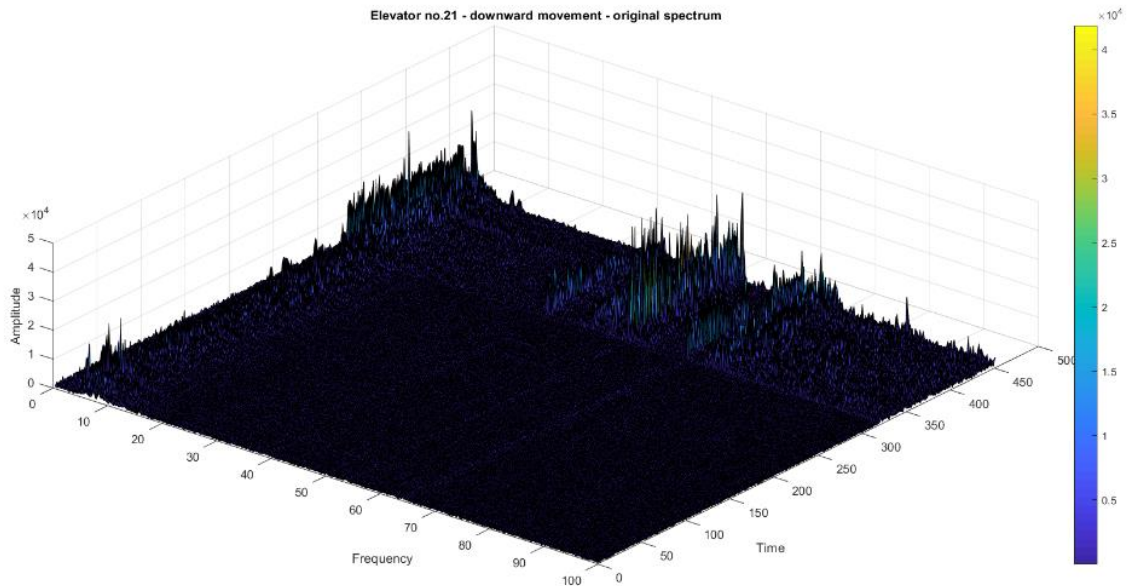
Figure 36.   *Original spectrum of elevator no. 21, downward movement.*

The change in vibration amplitude can be clearly seen by rotating the spectrum and view it from another angle. This is shown in Figure 37, together with a visual marking for the detected change point.
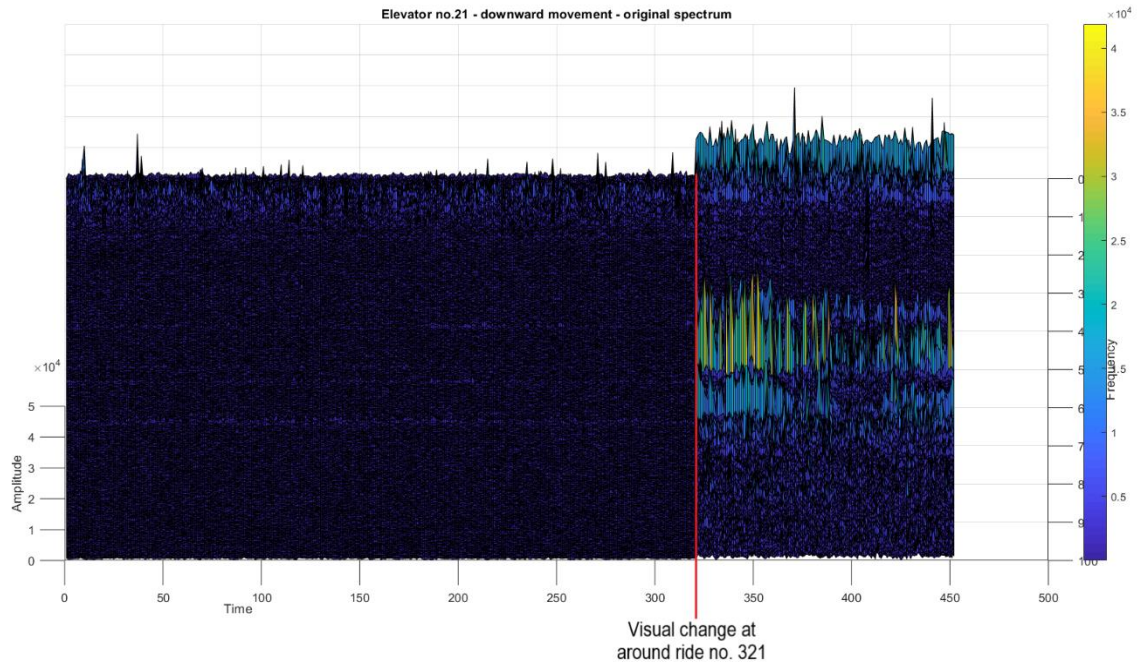
Figure 37.   *Visually detected change point for elevator no. 21, downward movement.*

Using feature selection, we can obtain the three most dominant frequencies of elevator no. 21, downward movement. Change point detection is then applied to find out if the change can be correctly detected or not. The results are shown in Figure 38.
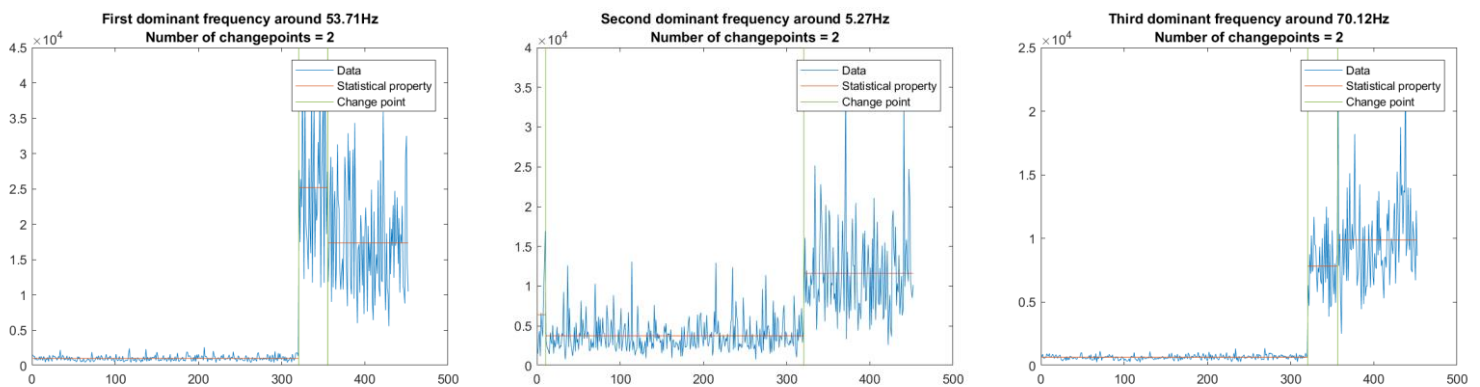
Figure 38.   *Results for change point detection of three most dominant frequencies of elevator no. 21, downward movement.*

Results from Figure 38 shows that the visible change at around ride no. 321 was precisely identified. The percentage change for first frequency (53.71Hz) was 2109.47%, for the second frequency (5.27Hz), it was 207.10% and lastly, 1100.49% for the third frequency (70.12Hz). These changes can also be considered to be very high, similar to upward movement. The required time for calculation was 0.67 seconds.

Using Autoencoder, two features of elevator no. 21, downward movement are extracted. Figure 39 shows the extracted features together with their respective change points.
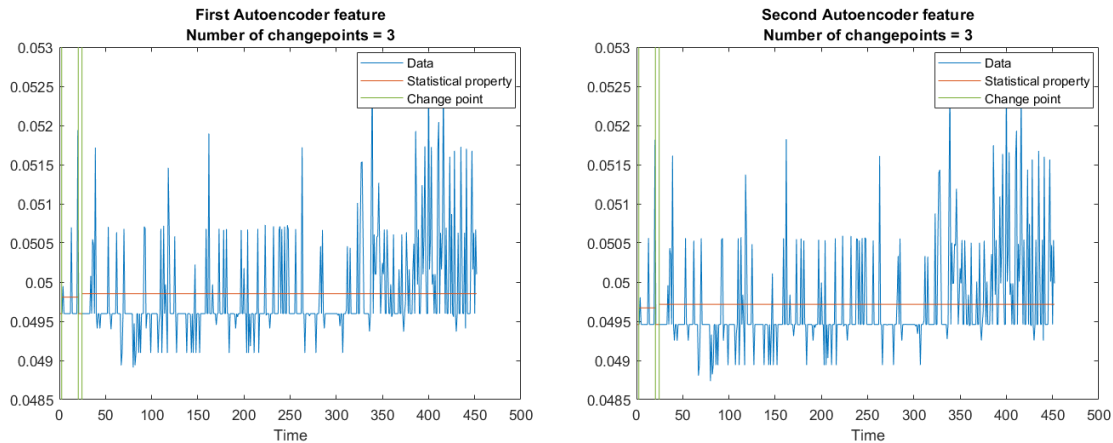
Figure 39.   *Result for change point detection of two extracted features (standard deviation) of elevator no. 21, downward movement.*

Once again, change point detection with *standard deviation* as statistical property did not detect the change correctly. Different results can be acquired using *mean* instead.

With different statistical property (*mean*), the new results for change point detection can be obtained. These are shown in Figure 40.
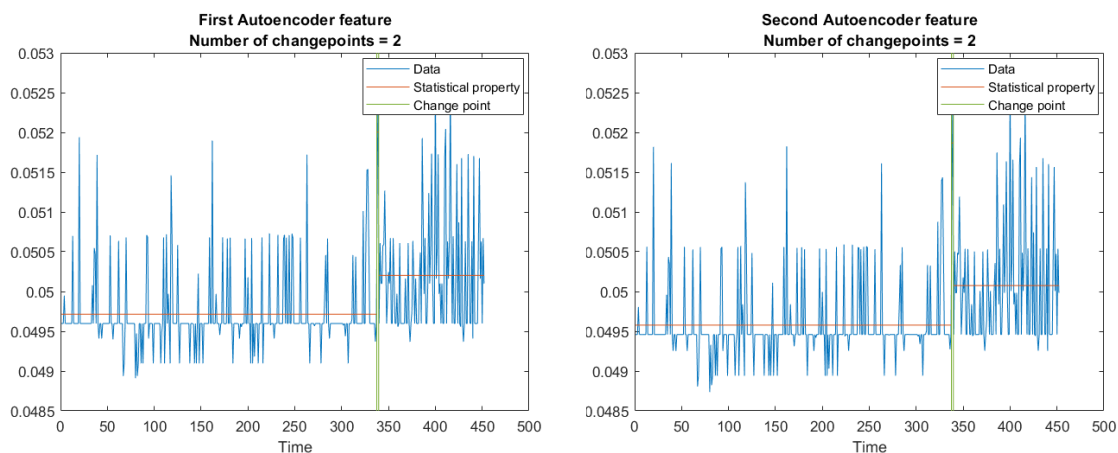
Figure 40.   *Result for change point detection of two extracted features (mean) of elevator no. 21, downward movement.*

As can be seen from Figure 40, the new results now have the change point at ride no. 338, closer to the expected change at around ride no. 321 compared to before. However, this is not as ideal as the difference is still quite large. The calculation time was 20.39 seconds.

Aside from adjusting the statistical property, other approaches can also be applied to improve the results. For this case of elevator no. 21, downward movement, we tried to increase the number of training epochs of Autoencoder to acquire a new set of extracted features. The first Autoencoder was trained for 600 epochs max and the second one was trained for 300 epochs.

By modifying the parameters further, we can acquire another set of results as displayed in Figure 41. The new features, as well as the change points detected, are quite different compared to Figure 40.
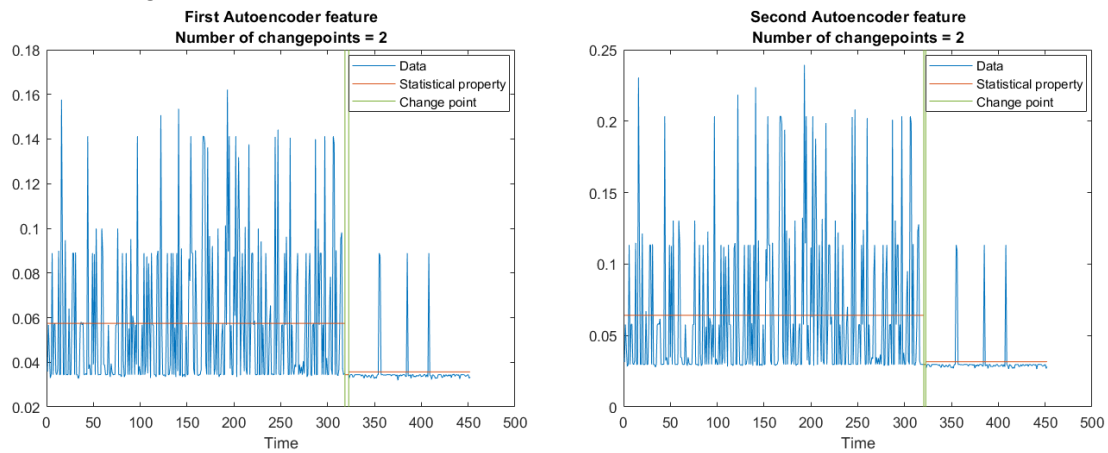
Figure 41.   *Result for change point detection of two extracted features (standard deviation and number of training epochs increased) of elevator no. 21, downward movement.*

From the results for the new set of extracted features in Figure 41, we can see that the change point at around ride no. 321 has now been successfully detected for the second feature. For the first feature, the change was spotted at ride no. 319. The new features also have a clearer visual difference in data before and after the change. Calculation time after the increase in training epochs also increased to 32.23 seconds.

Figure 42 shows the comparison between results attained from feature selection and feature extraction (with increased training epochs) against the visually detected one.
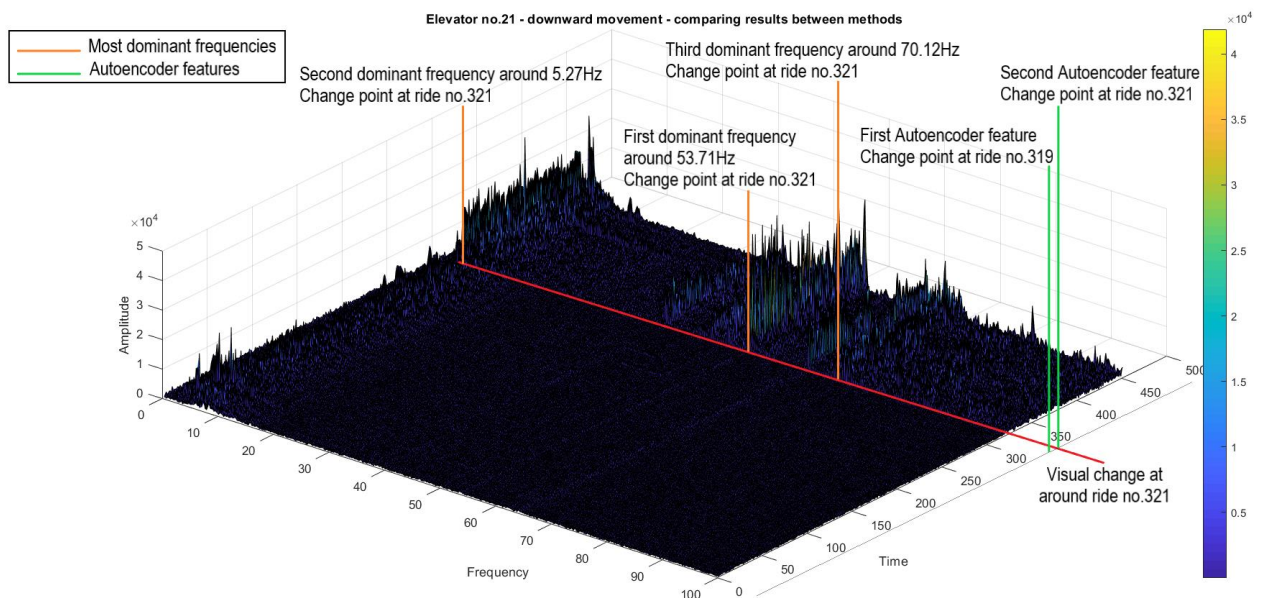
Figure 42.   *Comparison of change points detected for elevator no. 21, downward movement.*

In summary, for elevator no. 21, good performance continued to be shown by feature selection with dominant frequencies analysis and change point detection with statistical property being standard deviation. For feature extraction with Autoencoder, however, different default parameters need to be modified in order to attain satisfactory results. These changes include changing the statistical property and increasing the number of training epochs. The calculation time of feature extraction with Autoencoder is still much slower than feature selection.

4.3   Discussion

Above are the 4 selected cases of elevators with different characteristics. The first one is elevator no. 1 with no visible change in vibration amplitude. The second is elevator no. 14 with a noticeable but small change. Next is elevator no. 15 with both amplitude increase and decrease. The last one is elevator no. 21 with a large amplitude increase. In this work, all 29 elevators, both upward and downward movements have been inspected using the two techniques: feature selection with dominant frequencies analysis and feature extraction with Autoencoder.

Out of 29 elevators, there are 12 cases with noticeable changes in amplitude of vibration for both upward and downward movement. Table 1 and 2 contains the comparison of results for upward and downward movement respectively. For each elevator movement, first, the visual change point is estimated. After that, the closest acceptable change points of each frequency and feature from feature selection (dominant frequency analysis) and feature extraction (Autoencoder) are shown correspondingly. We consider a detected change point to be acceptable if it is within 2 rides from the visually estimated change point. Finally, the highest percentage changes calculated from both methods are displayed. The 2 tables are sorted by descending percentage change in mean amplitude of *feature selection*. For cases that required modification in default parameters like elevator no. 21, a (*) mark is placed to represent these changes.

Elevator	Estimated visual change point (ride no.)	Feature selection with dominant frequencies analysis			Feature extraction with Autoencoder		Highest percentage change in mean amplitude (Feature selection)	Highest percentage change in mean amplitude (Feature extraction)
		Change point 1st frequency (ride no.)	Change point 2nd frequency (ride no.)	Change point 3rd frequency (ride no.)	Change point 1st feature (ride no.)	Change point 2nd feature (ride no.)		
21	~221	221	221	221	221*	221*	1305.32% (3rd frequency)	26.63% (2nd feature)
27	~80	79	79	79	80	80	1196.7% (2nd frequency)	84.07% (1st feature)
8	~211	211	212	None	211*	211*	1008.04% (1st frequency)	10.82% (1st feature)
4	~89	None	89	None	89*	89*	569.23% (2nd frequency)	66.19% (2nd feature)
6	~161	161	161	None	161	161	567.64% (1st frequency)	59.22% (2nd feature)
28	~125	125	None	None	125*	125*	524.83% (1st frequency)	17.46% (2nd feature)
29	~220	220	220	220	220*	220*	520.89% (2nd frequency)	3.62% (2nd feature)
15	~12 and ~120	12 and 120	12 and 120	12 and 120	12 and 120	12 and 120*	403.26% (2nd frequency)	1582.80% (2nd feature)
9	~66	None	66	66	64*	64*	329.8% (2nd frequency)	3.17% (2nd feature)
14	~76	None	76	77	76	76	170.96% (2nd frequency)	53.57% (2nd feature)
13	~108	109	None	110	108	108	105.44% (3rd frequency)	62.00% (1st feature)
5	~101	None	101	101	101*	101*	93.18% (3rd frequency)	67.27% (1st feature)

Table 1. *Comparison of results for elevators with visual changes in vibration amplitude, upward movement.*

Elevator	Estimated visual change point (ride no.)	Feature selection with dominant frequencies analysis			Feature extraction with Autoencoder		Highest percentage change in mean amplitude (Feature selection)	Highest percentage change in mean amplitude (Feature extraction)
		Change point 1st frequency (ride no.)	Change point 2nd frequency (ride no.)	Change point 3rd frequency (ride no.)	Change point 1st feature (ride no.)	Change point 2nd feature (ride no.)		
21	~321	321	321	321	319*	321*	2109.47% (1st frequency)	54.20% (2nd feature)
8	~201	201	None	None	201*	201*	739.95% (1st frequency)	90.34% (1st feature)
28	~132	132	132	132	132*	132*	621.17% (2nd frequency)	67.88% (2nd feature)
29	~240	240	240	None	240	240	592.02% (2nd frequency)	1.48% (2nd feature)
6	~136	None	136	136	136*	136*	583.15% (2nd frequency)	36.36% (2nd feature)
4	~78	None	None	78	78*	78*	401.06% (3rd frequency)	16.60% (2nd feature)
9	~50	None	49	None	None	50*	178.89% (2nd frequency)	241.23% (2nd feature)
15	~14	14	None	14	None	14	163.12% (3rd frequency)	1231.43% (2nd feature)
5	~108	106	None	108	108*	108*	142.19% (3rd frequency)	5.82% (2nd feature)
13	~95	95	95	95	95	95	137.36% (3rd frequency)	3104.93% (2nd feature)
14	~57	56	None	57	None	56*	122.42% (3rd frequency)	83.19% (2nd feature)
27	~104	104	103	None	103*	103*	95.65% (1st frequency)	5.24% (2nd feature)

Table 2. *Comparison of results for elevators with visual changes in vibration amplitude, downward movement.*

As can be seen from the two tables, for feature selection with dominant frequencies analysis, if there existed changes in vibration amplitude within the spectrum, then the change point detection (standard deviation) would correctly detect those changes in at least one of the elevator's most dominant frequencies. Only for elevators no. 13 and no. 27, upward movement, and elevator no. 9, downward movement, that change point detection missed the estimated targets by 1 ride. However, as the difference in results is minimal, we can consider it to be within the acceptable range.

For feature extraction, even though Autoencoder can capture a good representation of the original spectrum when it comes to changes in amplitude, the default parameters need to be modified in numerous cases in order to achieve desirable results. Most of these are about changing the statistical property of change point detection, however, for some cases like elevator no. 21, the number of training epochs also needs to be changed. For elevators no. 9, upward movement, elevator no. 14 and no. 27, downward movement, change point detection missed the estimated target output by 2, 1, and 1 ride respectively. These results are also within the acceptable range.

When it comes to percentage change, we can see that the results for the two methods do not match. This is because the extracted features from Autoencoder are the new subset of data, and do not reflect the actual magnitude of changes from the original spectrum. Therefore, percentage change from feature selection should be the main indicator for detecting elevators with high increases in vibration amplitude. Using this information, we can accurately point out the four elevators with the highest percentage increase in vibration amplitude. In this case, they are elevators *no. 21, no. 27, no. 8* and *no. 4* for upward movement, and elevators *no. 21, no. 8, no. 28* and *no. 29* for downward.

As for cases of elevators without noticeable visual changes in vibration amplitude, we noticed that there are 2 cases with abnormally high percentage increases:

- Elevator no. 16, downward movement: 482% increase
- Elevator no. 18, downward movement: 162% increase
- Elevator no. 7, downward movement: 106.96% increase

Upon closer inspection, we can see that for elevator no. 16 downward movement, there are several parts of the spectrum that do not contain any relevant data and are represented by empty lines, as can be seen from Figure 43. These "blank" data sections were the cause for inaccurate detection of change points.
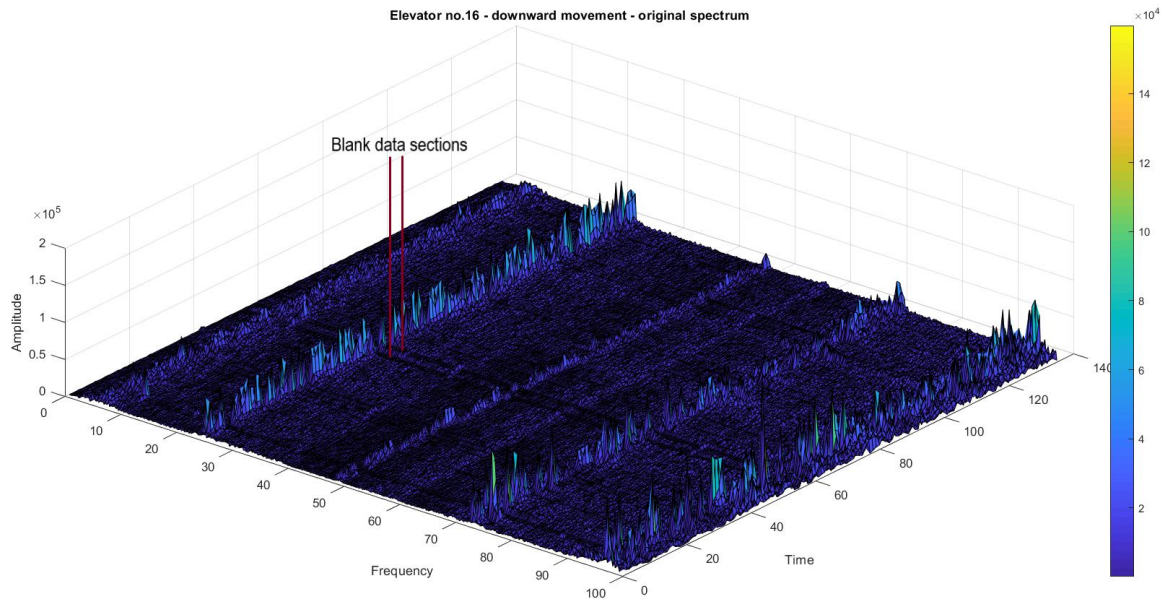
Figure 43.   *Blank data sections detected in elevator no. 16, downward movement.*

For elevator no. 18 downward movement, there are 2 high spikes, or outliers, in the spectrum, as can be observed from Figure 44, which increase the mean amplitude of the area and directly interfere with the change point detection algorithm. This serves as an example of how outlier can affect change point detection and requires more investigation in the future.
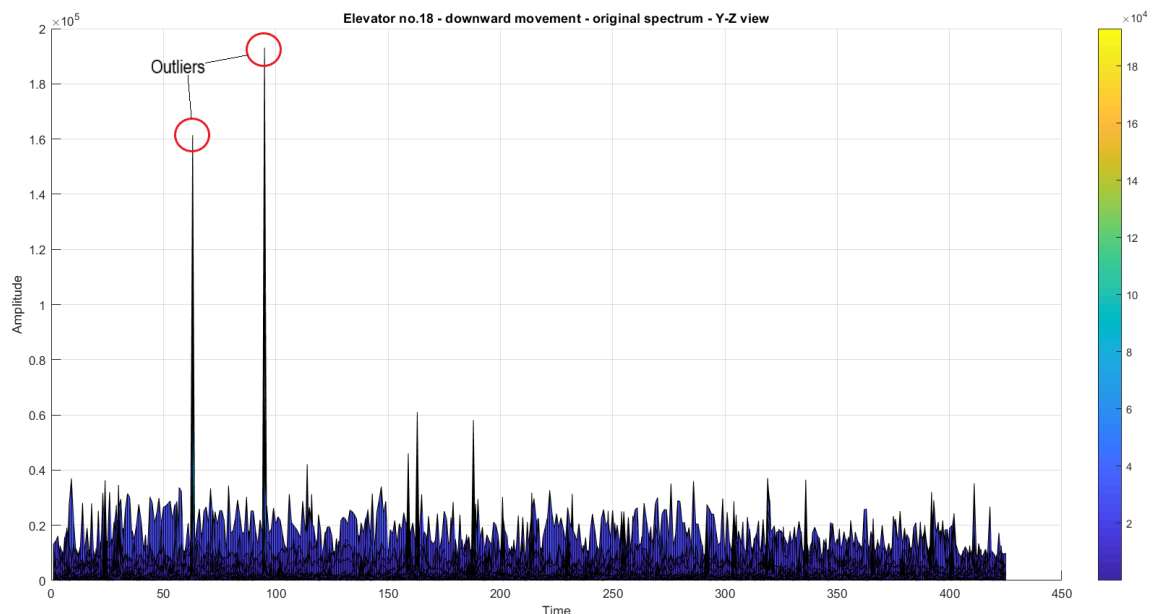
Figure 44.   *Abnormal high spikes, or outliers, in elevator no. 18, downward movement.*

For elevator no. 7, downward movement, we can see a huge deviation in high energy bins after each ride from Figure 45. We decided to increase the default window length from 5 to 9

and the maximum percentage increase went down to 28.16%. This was the only case where feature selection needed to modify its default parameters to obtain the expected results.
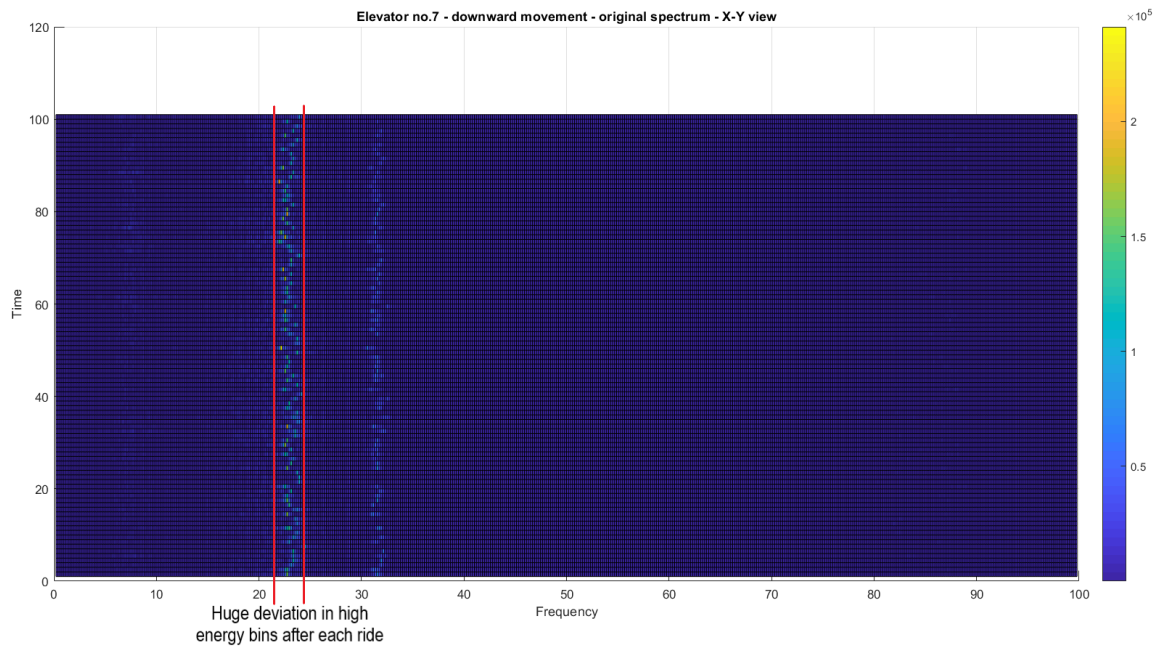
Figure 45. *Huge deviations in high energy bins after each ride in elevator no. 7, downward movement.*

As for the remaining cases of elevators without visual changes in vibration amplitude, in both feature selection and feature extraction, change point detection would either find no change point or the percentage change is marginal (maximum 71.27%) compared to cases that do have clear amplitude changes. The details for this can be found in the appendix tables.

All in all, from the acquired results, we can argue that:

- **For 12 elevator cases with noticeable changes in vibration amplitude**, both methods, feature selection and feature extraction, can deliver the same, accurate results when it comes to detecting the change points.
- **For the remaining cases without noticeable amplitude changes**, feature selection and feature extraction, together with change point detection struggle slightly due to missing or inconsistent data and outliers.

In terms of performance, feature selection with dominant frequencies analysis is much faster in computation time (5.51 seconds for upward movement and 5.54 seconds for downward) compared to feature extraction with Autoencoder (467.27 seconds for upward and 491.52 seconds for downward). Additionally, for several cases, Autoencoder requires changes in default parameters' values in order to produce acceptable results. Thus, feature extraction with Autoencoder might not be as efficient compared to feature selection in processing and detecting changes for the whole population of elevator.

5. CONCLUSION

This study was conducted to determine how FFT based features, or FFT data, could be used in fault detection and prediction in elevators. As the data is unsupervised and has high dimension, we decided to apply two techniques for data analysis: feature selection with dominant frequencies analysis and feature extraction with Autoencoder. After that, change point detection was used to determine the starting points of abnormal behaviors or anomalies and percentage change was calculated to find out which elevators had the highest increase in vibration amplitude.

Results have shown that the most dominant frequencies from feature selection using our method were successfully used in change point detection. For all cases where changes can be visually observed, the detection algorithm managed to correctly detect the change points. For more stable elevator system, the algorithm underperformed in 2 cases due to missing data and outliers' interference, and for the remainders, either no change point was detected or the percentage change in amplitude was determined to be small.

When it comes to feature extraction, even though Autoencoder did capture a good representation of the original spectrum, the default parameters need to be changed for several cases in order to acquire acceptable results. This approach also performed significantly slower than the dominant frequencies analysis in feature selection. For an automated system used on a large population of elevator, this might not be an ideal solution compared to feature selection.

Afterward, using the percentage change calculation, we were able to determine the most problematic elevators with the highest percentage increase in vibration amplitude. Using this information, the maintenance team can determine which one in a large population of elevator requires immediate attention and form a priority list for efficient maintenance schedule.

In conclusion, from this study, we can claim that FFT based features can be used in *detecting* potential faulty behaviors in elevator systems. Feature selection with dominant frequencies analysis and change point detection has shown promising results, accompanied by fast calculation time.

This master's thesis was a part of the OPENS Novel Predictive Analytics Technologies for Future Maintenance Business project, funded by Business Finland and industrial partners. For the university side, the partners are the Unit of Automation Technology and Mechanical Engineering from Tampere University and the Department of Computer Engineering from Åbo

Akademi University. The topic and orientation of this study were determined according to the OPENS objectives.

Future work:

For predicting elevator faults in a continuous stream of data, a sliding window could potentially be integrated into our algorithm. By doing this, we can recalculate the new features and use them in detecting new changes when they appear. Within the scope of the master thesis, we were not able to implement this feature into our system, however, it is possible to extend the idea for future development.

During the study, we have noticed that in some cases like elevator no. 18 downward movement, change point detection output incorrect results due to the outliers. We can obviously try to remove these outliers before applying change point detection, but this requires additional pre-processing and might not be efficient. However, in a recent study [32], P. Fearnhea and R. Guillem have proposed a different approach that is robust even in the presence of outliers by adapting the current penalized cost method. If we could analyze and implement this new technique, it would be a good improvement to our existing system.

As mentioned previously, going into detail about the individual components inside an elevator system is a very challenging task. However, if we can find out which frequency bin represents a specific component, it might be possible to prepare replacements beforehand without performing an on-site inspection to detect the faulty pieces. In our opinion, this would also be a valuable advancement for the current analysis work.

6. REFERENCES

[1]   United Nations Department of Economic and Social Affairs/Population Division, "World Urbanization Prospects 2018: Key Facts," 2018. [Online]. Available: http://www.apa.org/pubs/info/reports/2012-report.pdf. [Accessed 27 02 2019].

[2]   G. Niu, S.-S. Lee, B.-S. Yang and S.-J. Lee, "Decision fusion system for fault diagnosis of elevator traction machine," *Journal of Mechanical Science and Technology,* vol. 21, no. 1, pp. 85-95, 2008.

[3]   Markets and Markets, "Elevators and Escalators Market by Type & Service - Global Forecast 2021 | MarketsandMarkets," Markets and Markets, 8 2016. [Online]. Available: https://www.marketsandmarkets.com/Market-Reports/elevator-escalator-market-221792102.html. [Accessed 27 02 2019].

[4]   T. Ebeling, "Condition Monitoring for Elevators – An Overview," *Lift-Report,* p. 6, 2011.

[5]   I. Skog, I. Karagiannis, A. B. Bergsten, J. Härdén, L. Gustafsson and P. Händel, "A Smart Sensor Node for the Internet-of-Elevators—Non-Invasive Condition and Fault Monitoring," *IEEE Sensors Journal ,* vol. 17, no. 16, pp. 5198 - 5208, 2017 .

[6]   G. Betta, C. Liguori, A. Paolillo and A. Pietrosanto, "A DSP-based FFT-analyzer for the fault diagnosis of rotating machine based on vibration analysis," *IEEE Transactions on Instrumentation and Measurement,* vol. 51, no. 6, pp. 1316 - 1322, 2002.

[7]   I. Atoui, H. Meradi, R. Boulkroune, R. Saidi and A. Grid, "Fault detection and diagnosis in rotating machinery by vibration monitoring using FFT and Wavelet techniques," in *2013 8th International Workshop on Systems, Signal Processing and their Applications (WoSSPA)*, Algiers, Algeria, 2013.

[8]   S. S. Patil and J. A. Gaikwad, "Vibration analysis of electrical rotating machines using FFT: A method of predictive maintenance," in *2013 Fourth International Conference on Computing, Communications and Networking Technologies (ICCCNT)*, Tiruchengode, India, 2013.

[9]   S.-T. Park and B.-S. Yang, "An implementation of risk-based inspection for elevator maintenance," *Journal of Mechanical Science and Technology,* vol. 24, no. 12, p. 2367–2376, 2010.

[10]   J. Royo, R. Segui, A. Pardina, S. Nevot and F. J. Arcega, "Machine current signature analysis as a way for fault detection in permanent magnet motors in elevators," in *2008 18th International Conference on Electrical Machines*, Vilamoura, Portugal , 2008.

[11]   S. W. Smith, The Scientist and Engineer's Guide to Digital Signal Processing, California Technical Publishing, 1997.

[12]   E. W. Weisstein, "Fourier Series -- from Wolfram MathWorld," [Online]. Available: http://mathworld.wolfram.com/FourierSeries.html. [Accessed 27 02 2019].

[13]   V. Serov, Class Lecture, Topic: "Fourier series and the discrete Fourier transform." 802647S, College of Engineering and Science, University of Oulu, Oulu, 2014.

[14]   M. T. Heideman, D. H. Johnson and C. S. Burrus, "Gauss and the history of the fast Fourier transform," *Archive for History of Exact Sciences,* vol. 34, no. 3, p. 265–277, 1985.

[15]   G. D. Montanez, S. Amizadeh and N. Laptev, "Inertial Hidden Markov Models: Modeling Change in Multivariate Time Series," in *Twenty-Ninth AAAI Conference on Artificial Intelligence*, Austin, Texas, 2015.

[16]   S. Aminikhanghahi and D. J. Cook, "A survey of methods for time series change point detection," *Knowledge and Information Systems,* vol. 51, no. 2, p. 339–367, 2017.

[17]   R. Bellman, "Dynamic programming," *Science,* vol. 153, no. 3731, pp. 34-37, 1966.

[18]   Saroj and Jyoti, "Multi-objective genetic algorithm approach to feature subset optimization," in *2014 IEEE International Advance Computing Conference (IACC)*, Gurgaon, India , 2014.

[19]   G. James, D. Witten, T. Hastie and R. Tibshirani, An Introduction to Statistical Learning, Springer, 2013.

[20]   M. L. Bermingham, R. Pong-Wong, A. Spiliopoulou, C. Hayward, I. Rudan, H. Campbell, A. F. Wright, J. F. Wilson, F. Agakov, P. Navarro and C. S. Haley, "Application of high-dimensional feature selection: evaluation for genomic prediction in man," *Scientific Reports 5,* 2015.

[21]   R. Telgarsky, "Dominant Frequency Extraction," *arXiv preprint arXiv:1306.0103,* 2013.

[22]   T. Plante, L. Stanley, A. Nejadpak and C. X. Yang, "Rotating machine fault detection using principal component analysis of vibration signal," in *2016 IEEE AUTOTESTCON*, Anaheim, CA, 2016.

[23]   T. Junbo, L. Weining, A. Juneng and W. Xueqian, "Fault diagnosis method study in roller bearing based on wavelet transform and stacked auto-encoder," in *The 27th Chinese Control and Decision Conference (2015 CCDC)*, Qingdao, China, 2015.

[24]   W. Sun, S. Shao, R. Zhao, R. Yan, X. Zhang and X. Chen, "A sparse auto-encoder-based deep neural network approach for induction motor faults classification," *Measurement,* vol. 89, pp. 171-178, 2016.

[25]   K. Reddy, D. Rao, U.Ankaiah and K.Rajesh, "Handwritten Character and Digit Recognition Using Artificial Neural Networks," *International Journal of Advanced Research in,* vol. 3, no. 4, pp. 140-143, 2013.

[26]   S. Tangaro, R. Bellotti, F. D. Carlo and G. Gargano, "Digital Image Processing in Medical Applications, April 22, 2008," in *Applications of Mathematics in Models, Artificial Neural Networks and Arts*, Springer, Dordrecht, 2010, pp. 457-473.

[27]   C. Yves and D. E.Rumelhart, Backpropagation: theory, architectures, and applications., Psychology Press, 2013.

[28]   I. Goodfellow, Y. Bengio and A. Courville, "Autoencoders," in *Deep learning*, MIT Press, 2016, pp. 499-523.

[29]   B. A.Olshausen and D. J.Field, "Sparse coding with an overcomplete basis set: A strategy employed by V1?," *Vision Research,* vol. 37, no. 23, pp. 3311-3325, 1997.

[30]   A. Ng, Class Lecture, Topic: "Sparse autoencoder." CS294A, Stanford University, Stanford, California, 2011.

[31]   M. Lavielle, "Using penalized contrasts for the change-point problem," *Signal Processing,* vol. 85, no. 8, pp. 1501-1510, 2005.

[32]   P. Fearnhea and R. Guillem, "Changepoint Detection in the Presence of Outliers," *Journal of the American Statistical Association,* 2018.

[33]   Stanford Research Systems, "Dynamic Signal Analyzer - SR785," [Online]. Available: https://www.thinksrs.com/downloads/pdfs/catalog/SR785c.pdf. [Accessed 27 2 2019].

APPENDIX

Elevator	Highest percentage increase
16	71.27%
22	70.60%
17	58.18%
3	52.43%
12	37.59%
20	35.32%
19	32.48%
24	31.64%
10	23.32%
23	20.38%
1	14.70%
25	7.46%
26	5.81%
11	0.61%
2	0%
7	0%
18	0%

Table 3. *Highest percentage increase calculated for elevators without visual changes in vibration amplitude, upward movement.*

Elevator	Highest percentage increase
16	482.62%
18	162.31%
7	106.96%
1	61.43%
17	43.68%
19	37.42%
11	30.70%
20	30.49%
25	26.94%
10	25.32%
22	17.70%
23	13.51%
26	11.53%
24	11.42%
2	8.64%
12	7.73%
3	5.07%

Table 4. *Highest percentage increase calculated for elevators without visual changes in vibration amplitude, downward movement.*